New Phytologist

A zinc finger protein SlSZP1 protects SlSTOP1 from SlRAE1-mediated degradation to modulate aluminum resistance

Lei Zhang[1,2]*, Danhui Dong[1]*, Jinfang Wang[3], Zhirong Wang[1], Jiaojiao Zhang[1], Ru-Yue Bai[1], Xuewei Wang[1], Maria Del Mar Rubio Wilhelmi[4], Eduardo Blumwald[4] (iD), Na Zhang[1,5] and Yang-Dong Guo[1] (iD)

[1]College of Horticulture, China Agricultural University, Beijing 100193, China; [2]Institute of Vegetables and Flowers, Chinese Academy of Agricultural Sciences, Beijing 100081, China; [3]National Watermelon and Melon Improvement Center, Beijing Academy of Agricultural and Forestry Sciences, Beijing 100097, China; [4]Department of Plant Sciences, University of California, Davis, CA 95616, USA; [5]Sanya Institute of China Agricultural University, Sanya 572000, China

Authors for correspondence:
Na Zhang
Email: zhangna@cau.edu.cn

Yang-Dong Guo
Email: yaguo@cau.edu.cn

Summary

- In acidic soils, aluminum (Al) toxicity is the main factor inhibiting plant root development and reducing crops yield. STOP1 (SENSITIVE TO PROTON RHIZOTOXICITY 1) was a critical factor in detoxifying Al stress. Under Al stress, *STOP1* expression was not induced, although STOP1 protein accumulated, even in the presence of RAE1 (STOP1 DEGRADATION E3-LIGASE). How the Al stress triggers and stabilises the accumulation of STOP1 is still unknown.
- Here, we characterised SlSTOP1-interacting zinc finger protein (SlSZP1) using a yeast-two-hybrid screening, and generated *slstop1*, *slszp1* and *slstop1/slszp1* knockout mutants using clustered regularly interspaced short palindromic repeats (CRISPR) in tomato.
- *SlSZP1* is induced by Al stress but it is not regulated by SlSTOP1. The *slstop1*, *slszp1* and *slstop1/slszp1* knockout mutants exhibited hypersensitivity to Al stress. The expression of SlSTOP1-targeted genes, such as *SlRAE1* and *SlASR2* (*ALUMINUM SENSITIVE*), was inhibited in both *slstop1* and *slszp1* mutants, but not directly regulated by SlSZP1. Furthermore, the degradation of SlSTOP1 by SlRAE1 was prevented by SlSZP1. Al stress increased the accumulation of SlSTOP1 in wild-type (WT) but not in *slszp1* mutants. The overexpression of either *SlSTOP1* or *SlSZP1* did not enhance plant Al resistance.
- Altogether, our results show that SlSZP1 is an important factor for protecting SlSTOP1 from SlRAE1-mediated degradation.

Introduction

Aluminum (Al) is the most abundant metal in the Earth's crust, and it is highly abundant in agronomical soils. Al chemical forms are highly dependent on soil pH (Matsumoto *et al.*, 2015). When soil pH is < 5.0, the soluble form (Al^{3+}) is highly favoured, causing toxic effects that affect plant roots (Ryan *et al.*, 1992). Al^{3+} ions damage root tip cells, disturbing nutrient uptake and inhibiting root elongation and lateral root development (Poschenrieder *et al.*, 2008). In total, 40% of tropical fields are affected by acidic soils (Sanchez & Salinas, 1981), making Al detoxification of acid soils and the development of Al stress-tolerant crops a significant priority for agriculture (Kibria *et al.*, 2021).

When grown in the presence of high Al concentrations, plants secrete organic acids (malate, citrate and oxalate) into the rhizosphere to chelate and detoxify Al^{3+} (Ma *et al.*, 2001). TaALMT1 (Al-ACTIVATED MALATE TRANSPORTER 1), the first characterised malate transporter in wheat (*Triticum aestivum*), contributes to Al detoxification by secreting malate from the

roots (Sasaki *et al.*, 2004). *ALMT1* homologous genes have been also found in Arabidopsis, soybean, tomato, and cabbage (Hoekenga *et al.*, 2006; Liang *et al.*, 2013; Ye *et al.*, 2017; Zhang *et al.*, 2018). Similar to ALMT, some of the MATE (MULTIDRUG AND TOXIC COMPOUND EXTRUSION) transporters, such as SbMATE (sorghum), TaMATE (bread wheat) and BoMATE1 (cabbage), were reported to be involved in Al resistance by secreting citrate (Magalhaes *et al.*, 2007; Garcia-Oliveira *et al.*, 2014; Wu *et al.*, 2014). *STAR1* and *STAR2* (*SENSITIVE TO Al RHIZOTOXICITY*) encode bacterial-type ATP binding cassette (ABC) transporters that mediate the secretion of UDP-glucose to modify the cell wall, contributing to plant Al resistance (Huang *et al.*, 2009; Bose *et al.*, 2010). *ALSs* also encode ABC transporter-like proteins in Arabidopsis (AtALS1/3/5) and in rice (OsALS1) that contribute to plant resistance to Al (Larsen *et al.*, 2005; Bose *et al.*, 2010; Huang *et al.*, 2012; Zhu *et al.*, 2013). *STAR1* expression was activated by ASR1/ASR5, which have been reported as Al-resistance transcription factors in rice (Arenhart *et al.*, 2014).

STOP1, also known as ART1 (Al RESISTANCE TRANSCRIPTION FACTOR 1), is considered a key

*These authors contributed equally to this work.

Al-resistance transcription factor in many plant species (Iuchi *et al.*, 2007; Yamaji *et al.*, 2009; Ohyama *et al.*, 2013). STOP1 regulates the expression of genes associated with tolerance of plants to different stress conditions (Sadhukhan *et al.*, 2021). In Arabidopsis, *stop1* knockout mutants did not show *AtALMT1* and *AtMATE* induction in response to Al stress (Iuchi *et al.*, 2007; Liu *et al.*, 2009), supporting the critical role of STOP1 in plant organic secretion. In rice, ART1 regulates the expression of an established Al-tolerance network by regulating the expression of *STAR1/2*, *NRAT1* (*NRAMP ALUMINUM TRANSPORTER 1*), and *FRDL4* (*FERRIC REDUCTASE DEFECTIVE LIKE* 1; Huang *et al.*, 2009; Yamaji *et al.*, 2009; Xia *et al.*, 2010). Rice contains another copy of STOP1 that is the closest homologue of AtSTOP1 rather than ART1 (Fan *et al.*, 2016). In rice bean (*Vigna umbellata*) and wheat, *VuSTOP1* and *TaSTOP1-A* were found to be slightly induced by Al (Fan *et al.*, 2015). Whether STOP1-like proteins have evolved specific Al resistant pathway remains to be studied.

Although STOP1/ART1 bound to the promoters of the Al-resistance genes, rapidly activating their expression (Tsutsui *et al.*, 2011; Fan *et al.*, 2015; Zhang *et al.*, 2019), *STOP1/ART1* transcription is constitutive in Arabidopsis, rice and other plant species and was not activated by Al (Iuchi *et al.*, 2007; Yamaji *et al.*, 2009; Yokosho & Ma, 2015; Fan *et al.*, 2016). In Arabidopsis, STOP1 interacts with the F-box protein RAE1, forming a negative feedback loop in which STOP1 upregulates *RAE1* expression and RAE1 promotes the degradation of STOP1 through the ubiquitin 26S proteasome pathway (Zhang *et al.*, 2019). Interestingly, although STOP1 induces the increased *RAE1* expression, which in turn degrades STOP1, STOP1 still accumulates under Al stress. HPR1, a component of the THO/TREX complex, prompts STOP1 mRNA export from the nucleus to regulate STOP1 protein levels (Guo *et al.*, 2020). Fang *et al.* (2020) found that STOP1 protein stability can partly be influenced by SUMOylation. In addition, Tokizawa *et al.* (2021) demonstrated that the phosphatidylinositol-specific phospholipase C (PI-PLC) pathway was also involved in STOP1 nuclear accumulation and affected the early expression of *GDH1/2* (*GLUTAMATE-DEHYDROGENASE*; Huang, 2021; Tokizawa *et al.*, 2021). Therefore, the regulation of STOP1 protein accumulation is a complex process, and how STOP1 senses Al stress and accumulates during the stress episode is still largely unknown.

Tomato is one of the most important vegetables around the world and crop productivity is limited by Al when plants are grown in acidic soils. The expression pattern of the *MATE* gene family was analysed, but the roles of these *MATEs* in the plant response of Al stress have not been characterised (dos Santos *et al.*, 2017). Ye *et al.* (2017) reported that an indel in *SlALMT9* enhanced tomato Al resistance. Several Al-inducible *SlNACs* (*NAM*, *ATAF* and *CUC*) and *SlAAEs* (*ACYL-ACTIVATING ENZYME*) genes were reported using genome-wide analysis of *NAC* and *AAE* gene families (Jin *et al.*, 2020, 2021). Nonetheless, few studies have focused on the regulatory mechanisms associated with the response(s) of tomato to Al stress.

Here, we identified a mechanism associated with the accumulation and the stability of STOP1 under Al stress. We screened a yeast-two-hybrid (Y2H) library and identified *SlSZP1*, encoding a putative Al stress-induced C2H2-type protein. Our results indicate that SlSZP1 functions as the obligate dependent cofactor of SlSTOP1 to promote its accumulation under Al stress in tomato.

Materials and Methods

Primers and constructs

All the primers used for qRT-PCR and the constructions in this study are listed in Supporting Information Table S1. All the restriction enzymes were purchased from NEB (Beijing, China), and the infusion enzyme was obtained from Vazyme (Nanjing, China).

Plant materials, culture condition and transformation

Solanum lycopersicum cv Micro-Tom seeds under investigation here were bought from Ballhort (https://www.ballhort.com/) and propagated in a glasshouse under natural light condition at China Agricultural University, Beijing (39°56′N, 116°20′E).

All the plants used in the following experiments were germinated on half-strength Murashige and Skoog (½MS) medium in plates for 7–10 d. The seedlings were then transferred to a hydroponic system, supplied with standard Hoagland nutrient solution for another 3 d before treatment (Urbanczyk-Wochniak & Fernie, 2005). Growth conditions were set at 16 h : 8 h, 26°C : 18°C, light : dark (Urbanczyk-Wochniak & Fernie, 2005). Tobacco plants used for transient transformation were grown in the glasshouse under the same conditions as above.

For the generation of *slstop1* knockout plants, we fused two target sequences (Table S1) into the pYAO-hSpCas9 system (Yan *et al.*, 2015). To obtain *SlSZP1* mutants, three target sequences were fused into the pTRANS-210d system (Cermak *et al.*, 2017). For generating *SlSTOP1*- and *SlSZP1*-overexpressing lines, *SlSTOP1* or *SlSZP1* was fused into pCAMBIA-1305 driven by the *CaMV 35S* promoter. The constructs were introduced into Micro-Tom tomato using *Agrobacterium*-mediated transformation (Sun *et al.*, 2006). Genomic DNA of the candidate lines was amplified and sequenced to identify mutations using primers covering the target sites (Table S1).

cDNA cloning and sequence analysis of *SlSTOP1*

The full-length cDNAs, *SlSTOP1* (Solyc11g017140), *SlSZP1* (Solyc04g056320) and *SlRAE1* (Solyc10g076290) were obtained from Sol Genomics Network (Fernandez-Pozo *et al.*, 2015). MEGA 5.0 was used to generate phylogenetic trees.

For subcellular localisation assays, coding sequences without a stop codon for *SlSTOP1* and *SlSZP1* were cloned into pCAMBIA 1300, fused with GFP and driven by the *CaMV 35S* promoter (*35S:SlSTOP1-GFP*, *35S:SlSZP1-GFP*). The constructs were transformed into 4-wk-old tobacco leaves using *Agrobacterium*-mediated transformation. A transient gene expression experiment was performed as described previously (Zhang *et al.*, 2020). Fluorescence signals were detected after 3 d using confocal microscopy (Nikon Inc., Tokyo, Japan).

For transactivation assays, *SlSTOP1* was divided into four parts (*NTR1*, *NTR2*, *C2H2* and *CTR*) according to the conservation of the sequences. These sections for *SlSTOP1*, *SlSTOP1* and *SlSZP1* were fused with pGBK-T7, and named pGBKT7-NTR1, pGBKT7-NTR2, pGBKT7-C2H2, pGBKT7-CTR, pGBKT7-SlSTOP1 and pGBKT7-SlSZP1. All the constructs and the empty vector were transferred into the Y2H Gold yeast strain. The activation of transformants was identified according to the manufacturer's instructions (Clontech, Mountain View, CA, USA; Wang *et al.*, 2018).

The expression pattern assay

For different metal treatments, wild-type (WT) plants were exposed to 60 μM $AlCl_3$, 10 μM $LaCl_3$, 0.5 μM $CuCl_2$, 100 μM $ZnCl_2$, 20 μM $CdCl_2$ for 9 h (pH 4.7). For the time-course experiments, the WT plants were subjected to 60 μM Al in 0.5 mM $CaCl_2$ (pH 4.7) or 30 μM Al in modified Hoagland solution (0.8 mM $Ca(NO_3)_2$, 1.5 mM KNO_3, 0.75 mM $MgSO_4$, 0.1 mM K_2HPO_4, 50 μM FeEDTA, 11.6 μM H_3BO_3, 2.4 μM $MnSO_4$, 0.2 μM $ZnSO_4$, 0.1 μM $CuSO_4$, 0.1 μM Na_2MoO_4) for 0, 0.5, 1, 3, 6, 9, 12 or 24 h (pH 4.5). The bud, flower, leaf shoot and root were sampled from WT plants under normal conditions (pH 5.7). For Al dose treatments, the WT plants were subjected to 0, 10, 30, 60 and 90 μM Al for 9 h (pH 4.7). For cycloheximide (CHX) treatments, the WT plants were treated with 0 or 10 μM CHX for 1 h before 0 or 30 μM Al treatment in modified Hoagland solution for 9 h (pH 4.5). cDNA was synthesised using Prime Script™ RT reagent kit (TaKaRa, Osaka, Japan), and qRT-PCR was conducted using the Light Cycler 480 Real-Time PCR System and the following program: 95°C/30 s followed by 40× (95°C/10 s and 60°C 34 s), and the transcription level was normalised with *SlUBQ*.

Evaluation of Al sensitivity

Plants used for evaluating Al sensitivity were treated with a modified Hoagland nutrient solution supplied with 0 μM (pH 4.5) or 30 μM $AlCl_3$ (pH 4.5, a 6.9 μM free Al^{3+} activity calculated by GEOCHEM-EZ) for 10 d (Urbanczyk-Wochniak & Fernie, 2005; Shaff *et al.*, 2010), the solutions were changed for every 3 d. The primary roots were photographed and measured using ImageJ software. Relative root growth, used to reflect Al sensitivity, equals the percentage of root elongation with Al divided by elongation without Al treatment.

To measure the content of Al in roots, 3-wk-old plants were exposed to 0.5 mM $CaCl_2$ solution at pH 4.7 for 6 h and then transferred to the same solution containing 0 or 60 μM $AlCl_3$ for 12 h. Al content was measured as previously described (Ligaba-Osena *et al.*, 2017). In brief, roots were immersed in cold 0.5 mM citrate solution followed by rinsing several times with cold ddH_2O. The roots were then collected, dried and weighed. The dried roots were digested in a 1 : 1 $HNO_3/HClO_4$ solution and diluted with 2% HNO_3. We measured Al concentration in the diluted solution using inductively coupled plasma mass spectrometry (ICP-MS; PerkinElmer NexION300D, Waltham, MA, USA).

Here, 3-wk-old plants were also used for determining organic acids. The plants were pretreated with a 0.5 mM $CaCl_2$ solution at pH 4.7 for 6 h and then transferred to 50 ml of the same solution containing 0 or 60 μM $AlCl_3$ for 24 h. The lyophilised sample was dissolved in 1 ml ddH_2O. Organic acid concentrations were detected using the HPLC system (Agilent HPLC 1100 series, Palo Alto, CA, USA) as described previously (Singh *et al.*, 2009).

RNA-seq and analysis

Total RNA was extracted from 20-d-old WT, *slstop5-6* and *slszp22-1* mutant plants treated with 0 or 60 μM Al solution (pH 4.7). Three biological replicated samples were collected from each treatment and sequenced by Majorbio (Shanghai, China). BMA software package (Li & Durbin, 2009) and BOWTIE (Langmead *et al.*, 2009) were used to map clean reads against the tomato reference genome SL3.0 (Fernandez-Pozo *et al.*, 2015) and reference genes. Gene expression levels were quantified using the fragments per kilobase of transcript per million mapped reads (FPKM) calculation method and RSEM (Li & Dewey, 2011). Differentially expressed genes between groups were analysed using the Noiseq method (Tarazona *et al.*, 2011). All raw data and expression details for the genes can be accessed at the Gene Expression Omnibus (GEO) database with accession numbers GSE168433 and GSE201111.

Protein–DNA interaction assays

The C2H2 *cis*-elements on candidate downstream genes were predicted on the PLANTPAN3.0 website (Chow *et al.*, 2019). For yeast-one-hybrid (Y1H) assays, SlSTOP1 or SlSZP1 were cloned into the pGAD-T7 vector as the bait, 400-bp promoter fragments (containing the C2H2 *cis*-element) of *SlASR2* and *SlRAE1* were cloned into the pAbAi vector as prey. The prey vectors were transformed into the Y1H Gold strain and selected for basic aureobasidin A (AbA) content. The prey strains were then transformed with bait vector and grown on SD−Ura/−Leu medium with or without 200 μg/l AbA. Positive and negative control were used as described in the manufacturer's Y1H manual (Clontech).

For the electrophoretic mobility shift assay (EMSA), 60-bp promoter fragments with predicted C2H2 binding sites for *SlASR2* and *SlRAE1* were synthesised with or without biotin label (Sangon Biotech, Shanghai, China). SlSTOP1 or SlSZP1 were fused with MBP (Myelin Basic Protein) and then transformed into *Escherichia coli* (BL21) for protein purification. Electrophoretic mobility shift assay experiments were then performed using a chemiluminescent EMSA kit (GS009; Beyotime Biotechnology, Shanghai, China).

For luciferase (LUC)/Renillia luciferase (REN) assays, the 400-bp promoter fragments of *SlASR2* and *SlRAE1* were cloned into pGreenII 0800-LUC as reporters, whereas *SlSTOP1* and *SlSZP1* were cloned into pGreenII 62-SK as effectors. The paired reporter and effector were transiently co-expressed in 4-wk-old tobacco leaves using *Agrobacterium*-mediated transformation. Firefly and *Renilla* luciferase activity assays were then measured following the Dual-Luciferase Reporter Assay System (Promega)

with the GLOMAX 20/20 reader. The ratio of LUC to REN was used to reflect the transcriptional level of the promoter.

Protein–protein interaction assays

The Y2H cDNA library was constructed by OE biotech (Shanghai, China) In brief, 3-wk-old tomato plants were treated with 60 µM Al for 9 h (pH 4.7). RNA from roots were used to construct prey cDNA library according to the manufacturer's instructions (Invitrogen). SlSTOP1 lacking its activation domain was fused into pGBK-T7 as bait and then transformed into yeast Y2H Gold. The bait strain was mated with the prey library and the potential interacting proteins for SlSZP1 in transformants were identified by sequencing.

Y2H assays were performed according to the Y2H system (Clontech). *SlSTOP1* and *SlSZP1* were individually cloned into pGAD-T7. The inactivation domains of *SlSTOP1*, *SlRAE1* and *SlRAE1ΔF* were individually cloned into pGBK-T7. Then, the two paired constructs were co-transformed into Y2H Gold strain. Interacting proteins would allow the yeast to grow on SD−TLHA with X-α-gal medium.

For the bimolecular fluorescent complementation (BiFC) assays, *SlSTOP1* was fused with N-terminal GFP, whereas *SlSZP1* was fused with C-terminal *GFP*. This pair of constructs was transiently co-expressed in 4-wk-old tobacco leaves using *Agrobacterium*-mediated transformation. The florescence signal was detected using confocal microscopy (Nikon Inc.) after 3 d.

Luciferase complementation imaging (LCI) assays were conducted as described previously (Chen *et al.*, 2008). *SlSTOP1-nLUC*, *SlRAE1-NLuc*, *SlRAE1ΔF-NLuc*, *SlRAE1-CLuc*, *SlRAE1ΔF-CLuc*, *CLuc-SlSZP1*, *AtMYC-NLuc* and *AtJAZ9-CLuc* constructions were generated. The designed pair of constructs was infiltrated into different positions of the same 4-wk-old tobacco leaf. LCI images were taken with a charge coupled device (CCD) camera. *AtMYC-NLuc* and *AtJAZ9-CLuc* were set as positive controls. MG132 was used to inhibit the activation of 26S proteasome.

For co-immunoprecipitation (Co-IP) assays, *SlSTOP1-GFP*, *SlSTOP1-Flag*, *SlRAE1-GFP*, *SlRAE1ΔF-GFP*, and *Flag-SlSZP1* were constructed to determine the interaction. Paired constructs were infected into 5-wk-old tobacco leaves. After 3 d recovery, the total protein from the infected leaves was extracted with native lysis buffer as described previously (Munoz & Mar, 2018). Immunoprecipitation was performed according to the manufacturer's instructions with GFP-trap magnetic beads (Chromotek, Munich, Germany) or anti-Flag M2 magnetic beads (Sigma) and was eluted with glycine-elution buffer. Samples were analysed using western blot and GFP and Flag antibodies.

For pull-down assays, SlSTOP1-MBP, GST-SlRAE1 and SlSZP1-His were used for quantitative competition analysis. These proteins were produced in BL21 cells. The BL21 cells were cultured at 16°C overnight with the addition of 0.1 mM isopropyl β-D-1-thiogalactopyranoside (IPTG). Proteins were then purified with GST/His Ni-NTA agarose (Thermo Fisher, Waltham, MA, USA). SlSTOP1-MBP (0 or 2 µg) was then incubated with same amount of GST-SlRAE1 or GST in 5 ml of pull-down binding buffer (20 mM Tris–HCl, pH 7.5, 150 mM NaCl and 0.1% Nonidet P-40) for 1 h at 4°C. Competitor SlSZP1-His was added to the mixture, which was incubated for another 1 h at 4°C and the mixture was pulled down with GST agarose beads and eluted with sodium dodecyl sulphate (SDS) loading buffer. The samples were then used for westerns blot and detected with MBP, GST and His antibodies.

Western blots

Western blot analysis was conducted as described in the *Definitive guide to western blot* (Abcam, Cambridge, UK). All monoclonal primary antibodies and secondary antibodies used here were purchased from CoWin Biosciences (Beijing, China). The polyclonal antibody raised against SlSTOP1 was designed and generated by Abclonal (Wuhan, China).

Statistical analysis

Statistical significance tests were performed using the general Student's *t*-test (two-way). Data are shown as means $\pm$ SD, indicated in the figures by *, $P < 0.05$; **, $P < 0.01$; ***, $P < 0.001$.

Accession numbers

Sequence data in this article can be obtained from Sol Genomics Network with the following accession numbers: *SlSTOP1*, Solyc11g017140; *SlSZP1*, Solyc04g056320; *SlRAE1*, Solyc10g076290; *SlALS3*, Solyc10g085950.2; *SlMATE3*, Solyc01g008420.3; *SlASR2*, Solyc04g071580.3.

Results

SlSTOP1 is a homologue of *AtSTOP1* in tomato

SlSTOP1 (Solyc11g017140), cloned from tomato, is conserved and shares high similarity with other dicotyledon species (88% with NtSTOP1 (LOC107807704), 55% with AtSTOP1 (AT1G34370); Fig. S1a). *SlSTOP1* comprises a 1533-bp gene encoding a 510 amino acids protein that is localised at the nucleus (Fig. S1b). To determine its transcriptional activity, four sections of SlSTOP1 encoding: NTR1 (1–85 aa), NTR2 (86–236 aa), C2H2 (237–400 aa) and CTR (401–510 aa) and also its full length were cloned into the pGBKT7 expression vector. The results demonstrated that NTR1, CTR and the full length of SlSTOP1 displayed transcriptional activation, whereas two conserved regions (NTR2 and C2H2) did not (Fig. S1c). We also found that a SlSTOP1 homologous protein (Solyc06g065440, XP 010322757.2) sharing 50% similarity with SlSTOP1, but lacking a NTR and CTR region (Fig. S1d), did not show transcriptional activity in yeast (Fig. S1e). Altogether, these results indicated that *SlSTOP1* encodes a C2H2 zinc finger protein showing transcriptional activation at both N- and C-termini.

To assess *SlSTOP1* expression patterns, qRT-PCR was conducted for treatments with different metals (Al, La, Zn, Cu and Cd), different plant organs (bud, flower, leaf, shoot and root),

increasing treatment times (0, 0.5, 1, 3, 6, 9, 12 and 24 h), and increasing Al concentrations (0, 10, 30, 60 and 90 µM). The results showed that *SlSTOP1* was constitutively expressed under different metal treatments, different time durations of the treatments with Al and increasing Al concentrations (Fig. S1f,h,i). The highest *SlSTOP1* expression levels were found in roots, compared with the different plant organs (Fig. S1g). Together, the results obtained for *SlSTOP1* were consistent with those reported previously for *AtSTOP1* (Iuchi *et al.*, 2007).

SlSTOP1 interacts with SlSZP1

It has been shown previously that, in the presence of Al, AtSTOP1 activated the expression of Al-responsive genes; however, *AtSTOP1* expression appeared to be constitutive and was not induced by Al (Sawaki *et al.*, 2009). Similar results were seen in rice (Yamaji *et al.*, 2009) and tomato (Fig. S1h,i). We hypothesised that there might be a factor interacting with STOP1, contributing to maintain its stability. Therefore, we performed a Y2H screening to identify SlSTOP1-interacting proteins. The conserved region (86–400 aa) of SlSTOP1, fused to GAL4-BD, was used as a bait. In total, 100s of clones were obtained and sequenced and 16 copies were shown to be the same gene, named *SlSZP1* (Solyc04g056320) and encoding STOP1-INTERACTING ZINC-FINGER PROTEIN 1 (SZP1). The SlSTOP1-SlSZP1 interaction was then confirmed using point-to-point Y2H (Fig. 1a).

To validate the SlSTOP1–SlSZP1 interaction, we performed BiFC using SlSTOP1-NGFP and SlSZP1-CGFP in tobacco leaves. The results showed that SlSTOP1 and SlSZP1 interacted in the nucleus (Fig. 1b). The SlSTOP1–SlSZP1 interaction was further confirmed using LCI. *SlSTOP1-nLUC* and *cLUC-SlSZP1* were co-infiltrated into tobacco leaves and displayed luciferase (LUC) signals (Fig. 1c), confirming the SlSTOP1–SlSZP1 interaction *in planta*. Co-immunoprecipitation (Co-IP) also showed that SlSTOP1-GFP could be immunoprecipitated with Flag-SlSZP1 (Fig. 1d). All the above-described results confirmed the interaction between SlSTOP1 and SlSZP1 both *in vivo* and *in vitro*.

SlSZP1 encodes a putative aluminum-inducible transcription factor

SlSZP1 encodes a putative zinc-finger transcription factor of 373 amino acids comprising three C2H2 zinc-finger domains. *SlSZP1* is conserved in dicotyledon plants and has putative orthologues in main crops (Fig. 2a). *SlSZP1-GFP* transient expression in tobacco leaves indicated that SlSZP1 was localised in the nucleus (Fig. 2b). SlSZP1 showed transcriptional activation activity in the Y2H Gold yeast strain (Fig. 2c). Analysis of organ-specific *SlSZP1* expression showed that, like *SlSTOP1*, *SlSZP1* was highly expressed in the roots (Fig. 2e). Among the different metals, Al induced the highest *SlSZP1* expression levels (Fig. 2d). *SlSZP1* expression increased with Al in a time- and concentration-dependent manner (Fig. 2d,f,g). Taken together, these results indicated that SlSZP1 acts as a putative Al-inducible transcription factor.

## slstop1, slszp1 and slstop1/slszp1 double mutant are hypersensitive to Al stress

To assess SlSZP1 and SlSTOP1 functions, we used the CRISPR/Cas9 system (Yan *et al.*, 2015; Cermak *et al.*, 2017) to generate single *slstop1*, *slszp1* and double *slstop1/slszp1* knockout lines. After two generations, we obtained Cas9-free *slstop1*, *slszp1*, and *slstop1/slszp1* homozygous knockout lines named *slstop5-6*, *slstop6-11*, *slszp21-1*, *slszp22-3*, *slstop/slszp3-5* and *slstop/slszp6-3* (Fig. S2a). The knockouts were confirmed using sequencing (Fig. S2b) and are shown schematically in Fig. 3a,b. The indels in *SlSTOP1* and *SlSZP1* resulted in early translation termination, except in *slszp21-1* where it caused a 585-bp out of frame shift (Fig. 3a,b).

To compare the Al-resistance of WT and all mutant lines, the plants were exposed to solutions containing 0 µM/30 µM Al (pH 4.5) and the relative plant growth was assessed. Following 10 d of treatment, all mutants displayed hypersensitivity to Al, compared with the WT plants (Fig. 3c). No significant differences in root elongation, fresh weight and citrate secretion were found in plants grown under control conditions (Fig. 3d,e,g). In the presence of Al, root elongation and fresh weight of all mutants were inhibited significantly (Fig. 3d,e). The mutant lines secreted lesser amounts of citrate in the rhizosphere and accumulated higher Al levels in their roots under Al treatment (Fig. 3f,g). No significant differences were found between *slstop1*, *slszp1* and the double mutant lines (Fig. 3d–g). The results described above indicated that both SlSTOP1 and SlSZP1 play crucial roles in tomato Al tolerance.

SlSTOP1 regulates the expression of Al-responsive genes

The expression of many genes is regulated by STOP1 (Sawaki *et al.*, 2009; Zhang *et al.*, 2019). We performed RNA-seq to reveal SlSTOP1 downstream-regulated genes by comparing the differences in gene expression between WT and *slstop5-6* under control and Al stress conditions. In total, 42 genes were downregulated in the *slstop1* mutant, compared with WT plants grown under control conditions. Conversely, 14 genes were upregulated under Al stress (Fig. 4a; Table S2). The expression of these 14 genes was then normalised by $\log_{10}$FPKM and is shown in Fig. 4b. From these 14 genes, four genes, previously reported in Arabidopsis, cabbage and rice as Al responsible, namely *SlALS3* (Solyc10g085950.2), *SlMATE3* (Solyc01g008420.3), *SlRAE1* (Solyc10g076290.2), and *SlASR2* (Solyc04g071580.3), were chosen for further study (Sawaki *et al.*, 2009; Arenhart *et al.*, 2014; Wu *et al.*, 2014; Zhang *et al.*, 2019).

To determine whether these genes were targets of SlSTOP1, promoter fragments (1000 bp from the ATG start codon) were used to identify *cis*-elements using PLANTPAN3.0 (Chow *et al.*, 2019). The gene promoters were then divided into 1–3 fragments (Fig. S4a) and the fragments of each promoter were cloned into pAbAi and inserted into the Y1H Gold genome as bait strains. The bait strains, transformed with *AD-SlSTOP1*, were then grown on SD/−Leu/+200–300 µg/l AbA The bait strains *R3* of *SlRAE1* and *A3* of *SlASR2* survived under selective
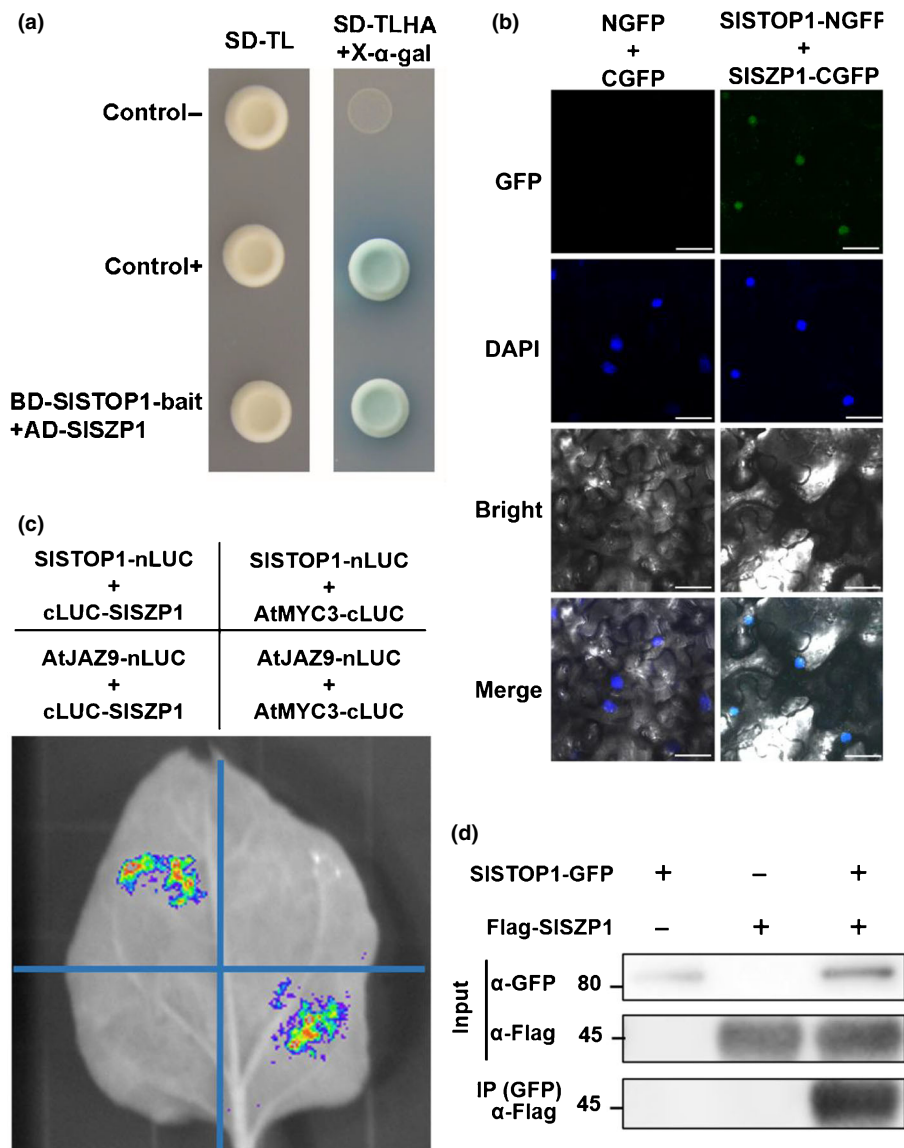
Fig. 1 Identification of the SlSTOP1 interacting protein SlSZP1. (a) Yeast-two-hybrid assay of SlSTOP1 and SlSZP1. STOP1-C2H2 was fused with GAL4-BD and co-transformed with SlSZP1 fused with GAL4-AD into Y2H Gold and grown on selection medium. Control+/Control− represent positive or negative controls. (b) Bimolecular fluorescent complementation (BiFC) assay of the interaction between SlSTOP1 and SlSZP1. SlSTOP1-NGFP and SlSZP1-CGFP were transiently expressed in tobacco leaves. NGFP and CGFP were set as negative controls. 4′,6-diamidino-2-phenylindole (DAPI) was used to visualise nuclei. Bar, 100 μm. (c) Luciferase complementation imaging (LCI) assay of interaction between SlSTOP1 and SlSZP1. Different areas of tobacco leaves were co-infiltrated with different pair constructs. SlSTOP1 and SlSZP1 were fused with nLUC and cLUC, respectively. AtJAZ9-nLUC and AtMYC3-cLUC were set as positive controls. (d) Co-immunoprecipitation (Co-IP) assay of the interaction between SlSTOP1 and SlSZP1. SlSTOP1-GFP, Flag-SlSZP1 or both were transiently expressed in tobacco leaves. Total protein was extracted, and immunoprecipitation was performed with anti-Flag antibody. Anti-GFP and anti-Flag were used to detect SlSTOP1-GFP and Flag-SlSZP1, respectively.

medium (Figs 4d, S3b), whereas the bait strains containing R1 and R2 of SlRAE1, A1 and A2 of SlASR2, promoters of SlMATE3 and SlALS3, did not (Figs 4d, S3b, S4b,c). These results indicated that SlSTOP1 could bind to SlRAE1 and SlASR2 promoters but not to SlMATE3 and SlALS3 in vitro. To confirm the binding of SlSTOP1 to the promoter of SlRAE1 and SlASR2, EMSA assays were performed with 60-bp fragments, containing the predicted C2H2 cis-element labelled with or without biotin or a C2H2 mutant probe (Figs 4c, S3a). The results showed that SlSTOP1 was able to bind to biotin-labelled DNA probes, but not the mutant probes (pRAE1 and pASR2). Also, the binding strength of SlSTOP1 decreased in the presence of unlabelled DNA probes (Figs 4e, S3c). Furthermore, we used R3 or A3 to drive LUC expression and co-infiltrated tobacco leaves with SlSTOP1 or 35S:Empty. The expression levels of R3:LUC and A3:LUC were three and five times higher, respectively, with SlSTOP1 compared with the empty vector (Figs 4f,g, S3d,e). Collectively, these results indicated that SlSTOP1 directly activated the expression of SlRAE1 and SlASR2 by binding to their promoters and indirectly induced the expression of SlMATE3 and SlALS3.

## Co-expression of SlSZP1 and SlSTOP1 enhances the expression of SlSTOP1 target genes

As SlSTOP1 interacts with SlSZP1, and the single mutants slstop1 or slszp1 and the double mutant slstop1 slszp1 showed a similar hypersensitivity to Al stress, we hypothesised that SlSZP1 may be involved in SlSTOP1-mediated Al-resistance pathway(s). We performed RNA-seq to reveal whether SlSZP1 regulated similar downstream-regulated genes as SlSTOP1 by comparing the differences in gene expression between WT and slszp22-1 under Al stress conditions. Compared with the WT, 1651 genes were downregulated (DRGs) in slszp22-1 and 1304 DRGs in slstop5-6, of which 448 were common to both slszp22-1 and slstop5-6 (Fig. 5a). Furthermore, 11 of the 14 core
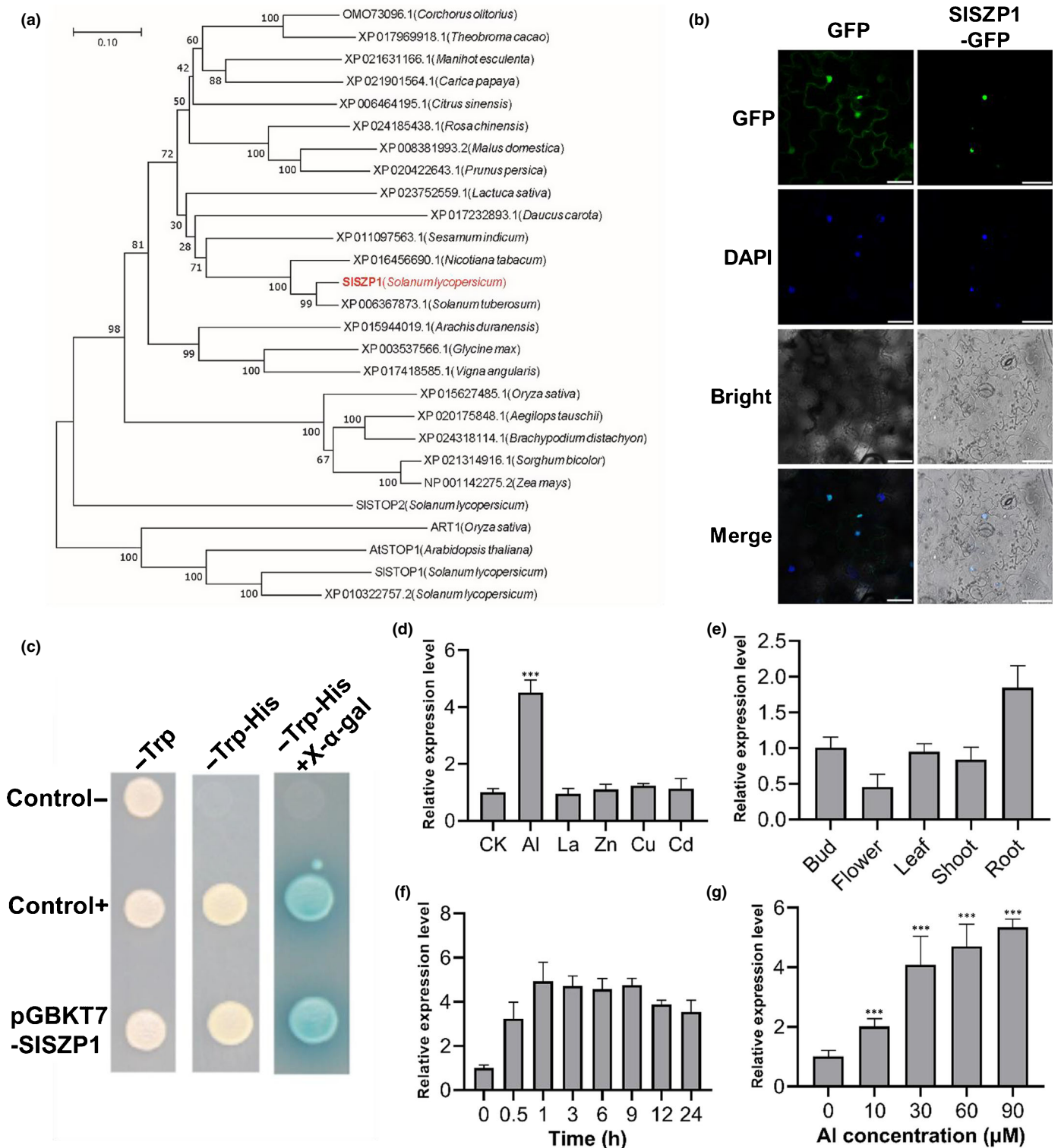
Fig. 2 Fundamental analysis of SlSZP1. (a) Phylogenetic tree of SlSZP1 in plants. SlSZP1 and its homologues and orthologues from various plants. Bootstrap values from 1000 replicates are indicated. The 0.10 scale represents the substitution distance. (b) Subcellular location of SlSZP1. SlSZP1-GFP was transiently expressed in tobacco leaves. 4′,6-diamidino-2-phenylindole (DAPI) was used to visualise nuclei. GFP was set as a mock control. Bar, 50 μm. (c) Transcriptional assay of SlSZP1 in yeast. Transformants with different constructs on selective medium. Control+/Control− represent positive or negative controls. (d–g) Expression patterns of SlSZP1. Two-week-old tomato plants, grown hydroponically, were treated with different metals (d), different time points (f), and different aluminum (Al) concentrations (g). Samples from different organs were collected from well flowering plants (e). Values are the mean ± SD ($n = 3$–4). Asterisks represent significant differences (t-test ***, $P < 0.001$).
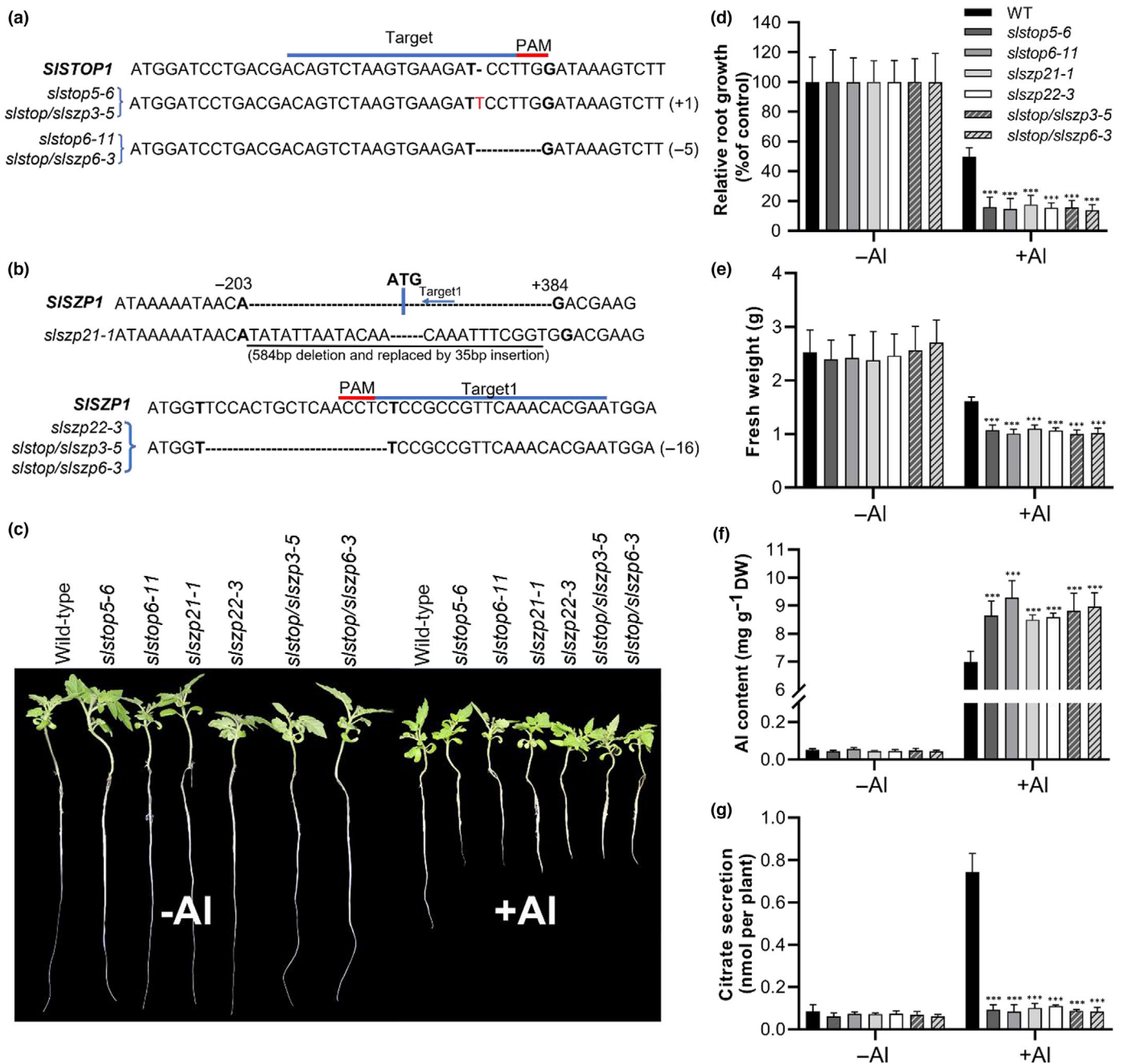
Fig. 3 Phenotype analysis of *slstop1*, *slszp1* and *slstop1/slszp1* mutants. (a, b) Schematic diagrams of *slstop1*, *slszp1 and slstop1/slszp1* mutants. (c–e) Phenotype image (c) and quantitative data (d, e) of wild-type (WT) and mutants. Here, 10-d-old plants were grown in Hoagland medium supplemented with 0 or 30 µM AlCl₃ (pH 4.5) for 10 d. Values are the mean ± SD (*n* = 8). (f, g) Aluminum (Al) content and citrate secretion in WT and mutants. Two-week-old plants were treated in 0 or 60 µM AlCl₃ solution for 12 h (f) or 24 h (g). Values are the mean ± SD (*n* = 3). Asterisks represent significant differences (*t*-test ***, *P* < 0.001).

SlSTOP1 downstream genes were among the common *DRGs* (Fig. 5b). These results indicated that SlSZP1 might be involved in plant Al resistance by regulating similar downstream genes as SlSTOP1. To test this hypothesis, we first assessed the expression levels of the SlSTOP1-regulated genes mentioned above in WT and all the mutant lines (Fig. 5c–f). Under control conditions, the expression of *SlASR2, SlALS3, SlMATE3* and *SlRAE1* were significant lower in all mutants compared with in WT plants, except for *SlMATE3* and *SlRAE1* in *slszp1* mutants. In

the presence of Al, the expression of *SlASR2, SlALS3, SlMATE3* and *SlRAE1* was significantly induced in WT and inhibited in all the mutants. We also found no statistical difference between mutant lines (Fig. 5c–f). In addition, *SlSTOP1* expression was not affected in the *slszp1* mutants, whereas *SlSZP1* expression was still induced by Al stress and displayed no significant difference between the WT and *slstop1* mutants (Fig. 5g,h). Moreover, we explored the expression of *SlSZP1, SlALS3,* and *SlRAE1* in WT plants in modified Hoagland solution
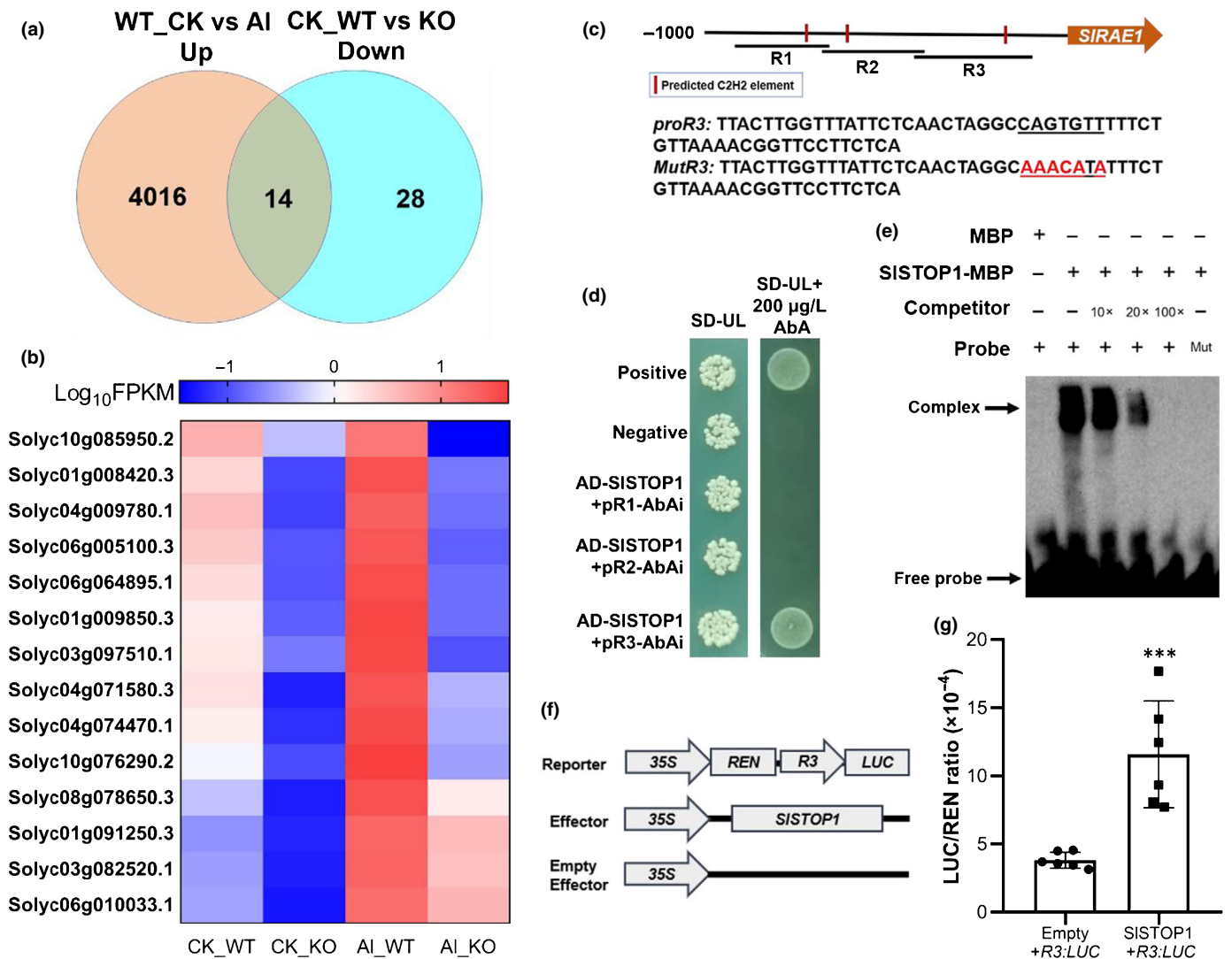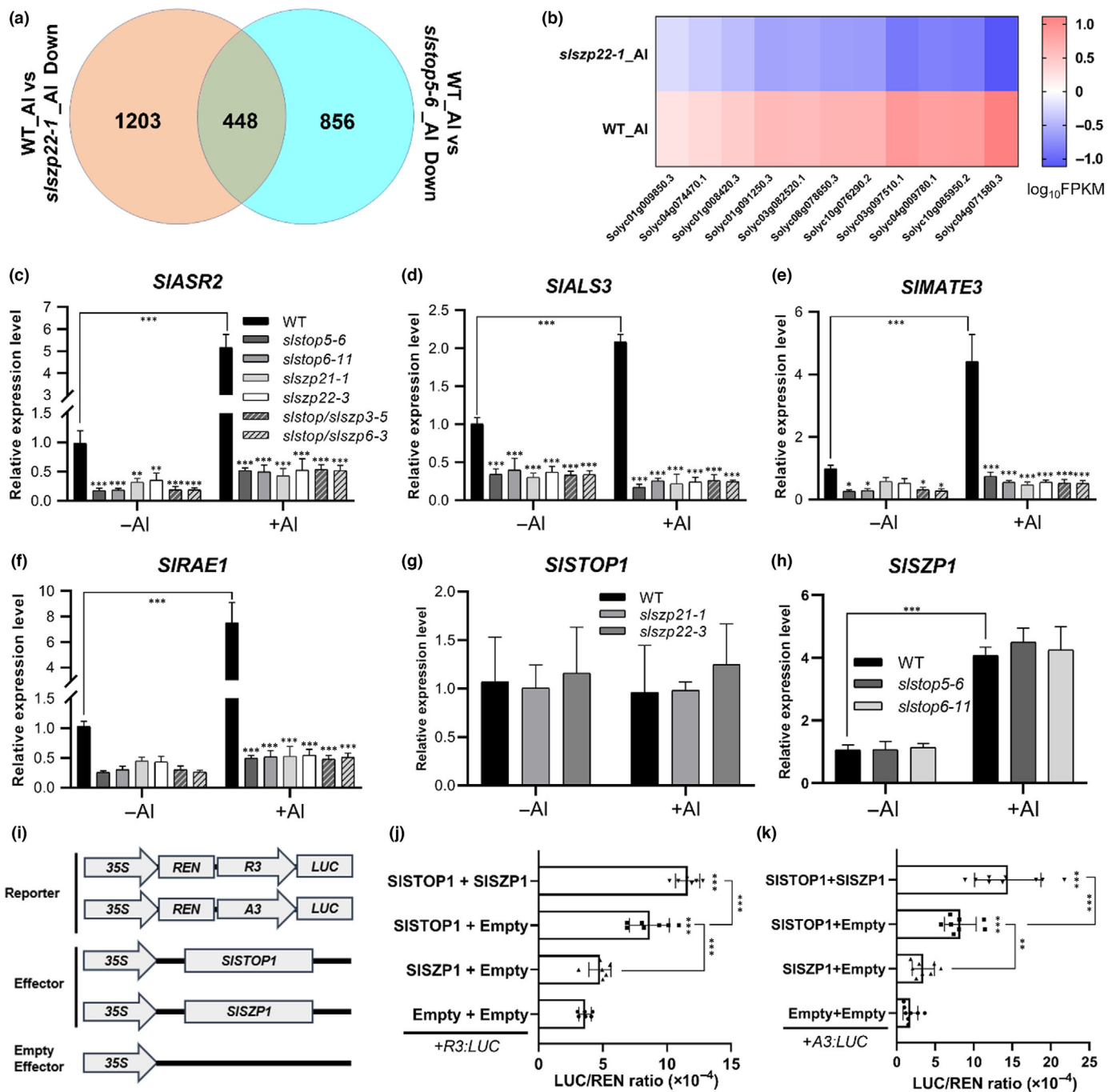
Fig. 4 SlSTOP1 regulates the expression of aluminum (Al) responsive genes. (a) Venn analysis of Al-responsive and SlSTOP1-regulated genes. Two-week-old plants were treated with/without 60 μM AlCl₃ for 9 h (pH 4.7). The roots were then sampled for RNA-seq. (b) Heatmap analysis of *slstop1* and Al-induced genes in WT and *slstop5-6* with/without 60 μM AlCl₃ for 9 h (pH 4.7). (c) Schematic diagram showing the promoter region and predicted C2H2 element of *SlRAE1*. R1–R3 indicate the fragment used in Y1H and LUC/REN assays. *proR3* and *MutR3* show the probe sequence used in the electrophoretic mobility shift assay (EMSA). Red text indicates mutant bases. The black underline indicates the promoter region of genes. (d) For yeast-one-hybrid assay, the promoter fragments of *SlRAE1* were cloned into pAbAi. The transformants with paired constructs were selected on SD−Ura/−Leu medium with or without suitable content of AbA. Positive and negative indicate the positive and negative controls. (e) For EMSA assays, *proR3* labelled with/without biotin and mutant probe were co-incubated with STOP1-MBP or with MBP for assays. (f, g) Schematic diagrams (f) of effector and reporter constructs used for LUC/REN assay (g). *SlSTOP1* was cloned into pGreen II 62-SK as the effector. The *R3* of *SlRAE1* was fused with the LUC gene as reporters. Promoter activities were reflected by the LUC : REN ratio. Empty vector (pGreen II 62-SK) + reporter was set as the control. The black squares and circles indicate different repeats. Values are the mean ± SD (*n* = 6). Asterisks represent significant differences (*t*-test ***, $P < 0.001$).

containing 30 μM Al (pH 4.5) and found that *SlSZP1* expression was rapidly induced in 0.5 h, whereas the expression of *SlALS3* and *SlRAE1* was induced after 6–9 h of Al treatment (Fig. S5a–c). We then used 0 or 10 μM cycloheximide (CHX) to treat WT for 1 h before Al treatment in modified Hoagland solution for 9 h (pH 4.5). The addition of CHX under Al stress conditions resulted in the inhibition of *SlSZP1* expression and influenced *SlALS3* and *SlRAE1* expression (Fig. S5d). Taken together, these results showed that SlSZP1 and SlSTOP1 might act as an upstream regulator to mediate plant Al tolerance through the same pathway.

To determine whether SlSZP1 could directly activate the expression of these four genes, we fused *SlSZP1* with pGADT7 and transformed it into the bait strains mentioned previously. SlSZP1 did not bind to any of the promoter fragments (Fig. S4d–g) and no activation was detected. When *SlSZP1* was co-infiltrated into tobacco leaves with *R3:LUC* / *A3:LUC* (Fig. 5i,k), SlSZP1 still did not show activation of *SlRAE1* and *SlASR2*. However, when both *SlSTOP1* and *SlSZP1* were co-infiltrated, *R3:LUC*/ *R3:LUC* was strongly activated and the LUC/REN ratio was higher than that seen with only *SlSTOP1* (Fig. 5j,k). Overall, the results indicated that SlSZP1 did not

Fig. 5 Co-expression of SlSZP1 and SlSTOP1 enhances the expression of SlSTOP1 target genes. (a) Venn analysis of downregulated genes (*DRGs*) in *slszp22-1* and *slstop5-6* compared with wild-type (WT) under aluminum (Al) stress conditions. Two-week-old plants were treated with 60 μM AlCl$_3$ for 9 h (pH 4.7). Roots were then sampled for RNA-seq. (b) Heatmap analysis of 11 SlSTOP1 downstream genes in WT and *slszp22-1* with 60 μM AlCl$_3$ for 9 h (pH 4.7). (c–h) Gene expression in WT, *slstop1*, *slszp1* or *slstop1/slszp1* mutants. RT-PCR was used to determine the expression of *SlASR2* (c), *SlALS3* (d), *SlMATE3* (e), *SlRAE1* (f), *SlSTOP1* (g) and *SlSZP1* (h) in the roots of 2-wk-old plants treated with/without 60 μM AlCl$_3$ for 9 h (pH 4.7). Values are the mean ± SD (*n* = 3–4). Asterisks represent significant differences (*t*-test *, *P* < 0.05; **, *P* < 0.01; ***, *P* < 0.001). (i–k) Schematic diagrams (i) of effector and reporter constructs used for the LUC/REN assay (j, k). *SlSTOP1* or *SlSZP1* were cloned into pGreen II 62-SK as effectors. The *proR3 of SlRAE1* (j) and *proA3 of SlASR2* (k) were fused with LUC gene as reporters. The paired effector and reporter were co-transformed into tobacco leaves. Promoter activities were reflected by the LUC : REN ratio. Empty vector (pGreen II 62-SK) + reporter was set as the control. The black squares and circles indicate different repeats. Values are the mean ± SD (*n* = 6–9). Asterisks represent significant differences (*t*-test *, *P* < 0.05; **, *P* < 0.01; ***, *P* < 0.001).

have the ability to bind to the promoter of SlSTOP1 target genes and that it modulated plant Al tolerance through its interaction with SlSTOP1.

SlSZP1 rescues SlSTOP1 from degradation by SlRAE1 under Al stress

It has been previously shown that in Arabidopsis, AtSTOP1 targeted AtRAE1, a F-box E3 ligase, capable of degrading AtSTOP1 through the ubiquitin pathway (Zhang *et al.*, 2019). Here, *SlRAE1*, an *AtRAE1* homologue, was also activated by SlSTOP1 (Fig. 4g). To assess whether SlSTOP1 could be degraded by SlRAE1, we used a yeast-two-hybrid assay to assess the interaction between SlSTOP1 and SlRAE1. The results showed that SlSTOP1 did not interact with full-length SlRAE1 (Fig. S6a), possibly due to the operation of the ubiquitin-mediated degradation in yeast. We constructed *BD-SlRAE1ΔF* (SlRAE1 without the F-box domain) and co-transferred it into the Y2H Gold with *AD-SlSTOP1*. The interaction between SlSTOP1 and SlRAE1ΔF was then detected (Fig. S6a). Also, LCI assays indicated an interaction between SlSTOP1 and SlRAE1ΔF, but not with SlRAE1 (Fig. S6c). Similarly to SlSTOP1, SlSZP1 is also a putative C2H2 type transcription factor, we hypothesised that SlSZP1 could also be degraded by SlRAE1. The same designed Y2H and LCI assays as described previously were conducted. Our results showed that SlSZP1 interacted with SlRAE1ΔF but not with SlRAE1 in yeast and in tobacco leaves (Fig. 6a,b). To evaluate the interaction between SlSTOP1 and SlRAE1, we co-infiltrated *Flag-SlSTOP1*, *Flag-SlSTOP1 + SlRAE1-GFP* or *Flag-SlSTOP1 + SlRAE1ΔF-GFP* into tobacco leaves and used Co-IP. The results showed that Flag-SlSTOP1 could be immunoprecipitated with SlRAE1-GFP/SlRAE1ΔF-GFP, and that the interaction between Flag-SlSTOP1 and SlRAE1-GFP was much weaker than the interaction between Flag-SlSTOP1 and SlRAE1ΔF-GFP (Fig. S6b). Similar experiments were also carried out to test the interaction between SlSZP1 and SlRAE1. Flag-SlSZP1 was also able to interact with SlRAE1-GFP (albeit weakly) and SlRAE1ΔF-GFP (Fig. 6c). To assess whether SlSTOP1/SlSZP1 was degraded through the 26S proteosome pathway, we performed an LCI assay with or without a MG132 injection, 6 h before observation. The SlSTOP1–SlRAE1 or SlSZP1–SlRAE1 interaction was only detected after the addition of MG132 (Fig. 6d). The results confirmed that both SlSTOP1 and SlSZP1 interacted with SlRAE1 *in planta* and that the interactions could be detected with the F-box-deleted SlRAE1. Therefore, SlRAE1 functions as an E3-ligase, promoting the degradation of SlSTOP1 and SlSZP1.

We hypothesised that SlSZP1 might protect SlSTOP1 from degradation by SlRAE1. To assess this hypothesis, we co-infiltrated *SlSTOP1*, *SlSZP1* or both, in tobacco leaves and performed LCI assays. LUC signals were not detected in *SlSTOP1* or *SlSZP1* combined with *SlRAE1* but were detected in the combination of *SlSTOP1-nLUC+ cLUC-SlSZP1+ SlRAE1-cLUC* and *SlSTOP1-nLUC+ cLUC-SlSZP1+ AtMYC-cLUC*, but not in *SlSTOP1-nLUC+ SlRAE1-cLUC+ AtMYC3-cLUC* and *cLUC-SlSTIP1+ SlRAE1-nLUC+ AtMYC3-cLUC* (Fig. 6e). These

results indicated that SlSTOP1 or SlSZP1 could not accumulate in the presence of SlRAE1. We examined whether SlSZP1 could hinder the interaction between SlRAE1 and SlSTOP1. Pull-down assays were conducted with SlSTOP1-MBP, GST-SlRAE1 and SlSZP1-His. SlSTOP1-MBP was preincubated with GST-SlRAE1 and then SlSZP1-His was used as a competitor. SlSTOP1-MBP was then pulled down using GST-SlRAE1. The results showed that the SlSTOP1–SlRAE1 binding weakened with increasing amounts of SlSZP1-His, indicating that the binding affinity of SlSZP1 to SlSTOP1 was higher than that of SlSTOP1 to SlRAE1 (Fig. 6f). To further determine whether SlSZP1 influenced the accumulation of SlSTOP1 under Al stress in tomato, we treated the roots of WT, *stop5-6* and *szp21-1* lines with or without 60 μM Al. The root proteins were then extracted and detected using antibodies raised against SlSTOP1. SlSTOP1 accumulated with the addition of Al, however, SlSTOP1 was not detected in *slstop1* mutants, and a weak signal was detected in *szp21-1* roots under both control and Al treatment conditions (Fig. 6g). These results would indicate that the interaction between SlSZP1and SlSTOP1 contributed to maintain the accumulation of SlSTOP1 under Al stress.

Overexpression of *SlSTOP1* or *SlSZP1* does not enhance tomato Al resistance

To further understand the role of SlSZP1 in tomato Al-resistance and on the maintenance of SlSTOP1 stability, we generated lines overexpressing *SlSTOP1* (*SlSTOP1-OE*) and *SlSZP1* (*SlSZP1-OE*) lines (Fig. 7a,b). Compared with WT, *SlASR2* and *SlRAE1* expression was not significantly induced in *SlSTOP1-OE* lines in the absence or presence of Al (Fig. 7c,d). Interestingly, *SlASR2* and *SlRAE1* expression was significantly induced in *SlSZP1-OE* lines in the absence of Al, but the differences disappeared in the presence of Al (Fig. 7c,d). Moreover, neither *SlSTOP1-OE* nor *SlSZP1-OE* lines displayed increased Al stress tolerance, which was consistent with the lack of difference in the expression of *SlASR2* and *SlRAE1* (Fig. 7c–f).

Furthermore, we detected the accumulation of SlSTOP1 in WT, *SlSTOP1-OE5* and *SlSZP1-OE4* lines under normal and Al stress conditions. The accumulation of SlSTOP1 in *SlSTOP1-OE5* was like that in the WT under both −Al and +Al conditions. In the absence of Al, the SlSTOP1 contents were lower in the WT and *SlSTOP1-OE5* (Fig. 7g) compared with that in *SlSZP1-OE4*. Under Al stress conditions, the SlSTOP1 contents were similar in the WT, *SlSTOP1-OE5* and *SlSZP1-OE4* lines. These results indicated that SlSZP1 contributed to SlSTOP1 stability even under Al stress conditions. Due to the presence of SlRAE1 and low amounts of SlSZP1, the overexpressed SlSTOP1 may not be stabilised by SlSZP1 and then is degraded by SlRAE1 (Fig. 7b,d,g).

Discussion

Previous studies have shown that AtSTOP1 plays significant roles in Al tolerance (Iuchi *et al.*, 2007; Ohyama *et al.*, 2013). Here, we cloned *SlSTOP1*, a homologue of *AtSTOP1* and *OsART1*,
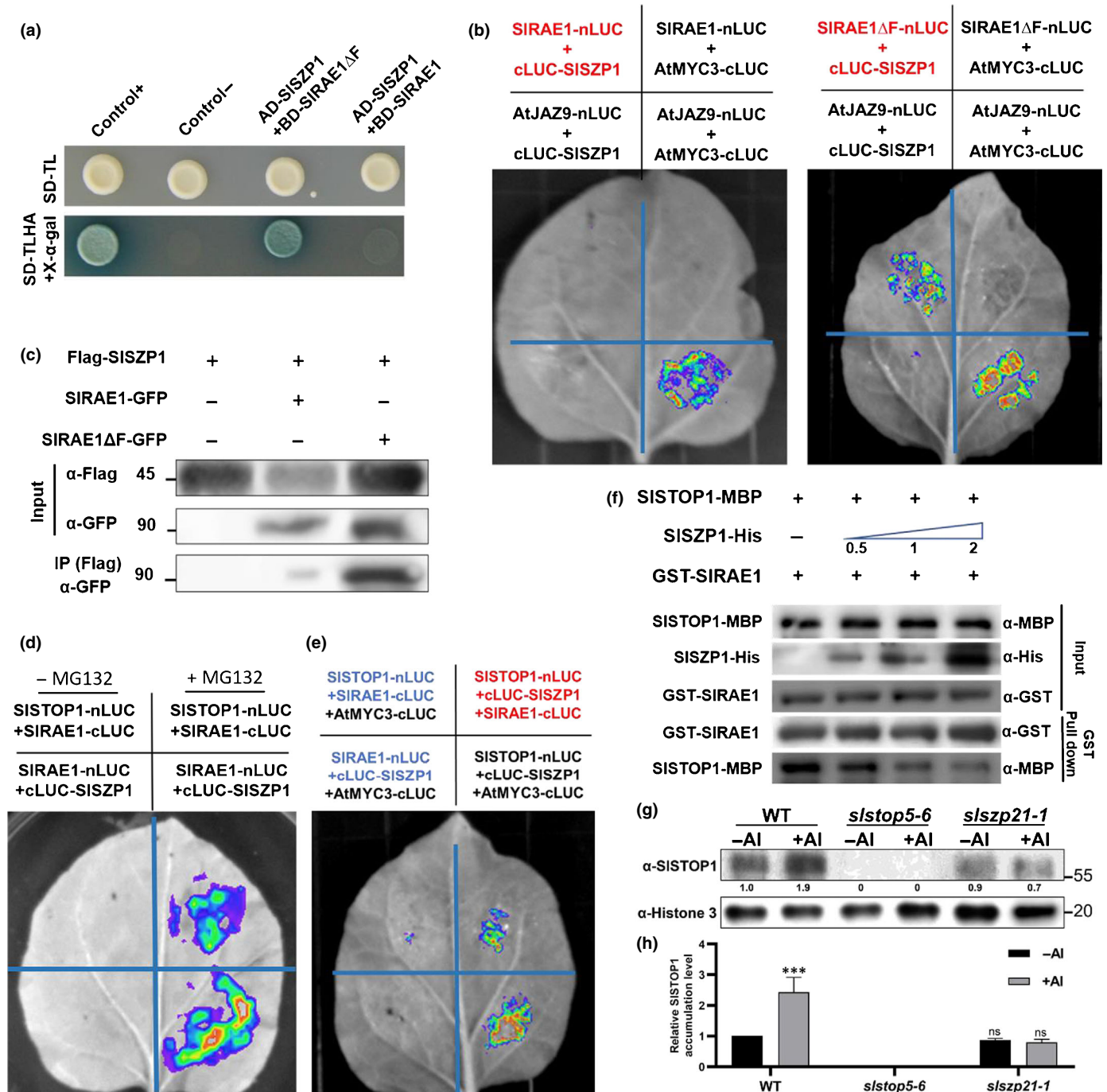
Fig. 6 SlSZP1 rescues SlSTOP1 from digestion by SlRAE1 under aluminum (Al) stress conditions. (a) For the yeast-two-hybrid assay, *SlSZP1* were fused with *GAL4-AD* and co-transformed with *SlRAE1/SlRAE1ΔF* fused with *GAL4-BD* into Y2H Gold and grown on selection medium. Control+/Control− represent positive or negative controls. (b) For the luciferase complementation imaging (LCI) assay, SlSZP1 were fused with N-terminal cLUC. SlRAE1 or SlRAE1ΔF was fused with nLUC. Different areas of tobacco leaves were co-infiltrated with different paired constructs. AtJAZ9-nLUC and AtMYC3-cLUC were set as positive controls. Red text represents experimental groups. (c) Co-immunoprecipitation (Co-IP) assay of the interaction between SlSZP1 and SlRAE1. Total protein in tobacco leaves expressing Flag-SlSZP1 with SlRAE1-GFP or SlRAE1ΔF-GFP was extracted, and immunoprecipitation was performed with the anti-Flag antibody. Anti-GFP and anti-Flag were used to detect Flag-SlSZP1, SlRAE1-GFP or SlRAE1ΔF-GFP. (d, e) SlSTOP1 was fused with nLUC, SlSZP1 was fused with cLUC and SlRAE1 was fused with nLUC or cLUC. Different areas of tobacco leaves were co-infiltrated with different paired constructs. MG132 was injected into a half part of tobacco leaves (d) 6 h before observation. Red text represents the experimental groups, and blue text represents the control groups. (f) *In vitro* pull-down assay to access the competition between SlSZP1 and SlRAE1 in binding to SlSTOP1. SlSTOP1-MBP was premixed with GST-SlRAE1, and the indicated gradient amounts of competitor SlSZP1-His were added to the mixtures. GST beads were then used for pull down, and the pellet was examined using immunoblot with anti-MBP antibody. (g, h) Five-week-old plants were treated with or without 60 μM AlCl$_3$ for 9 h. The roots were sampled for nucleoprotein extraction. The same amount of crude protein was then detected using antibodies raised against SlSTOP1 and Histone 3 (g). The experiment was repeated three times, and the SlSTOP1 accumulation was counted using IMAGEJ software and normalised with Histone 3 (h). Values are the mean ± SD ($n = 3$). 'ns' indicates no significant difference. Asterisks represent significant differences (*t*-test ***, $P < 0.001$).
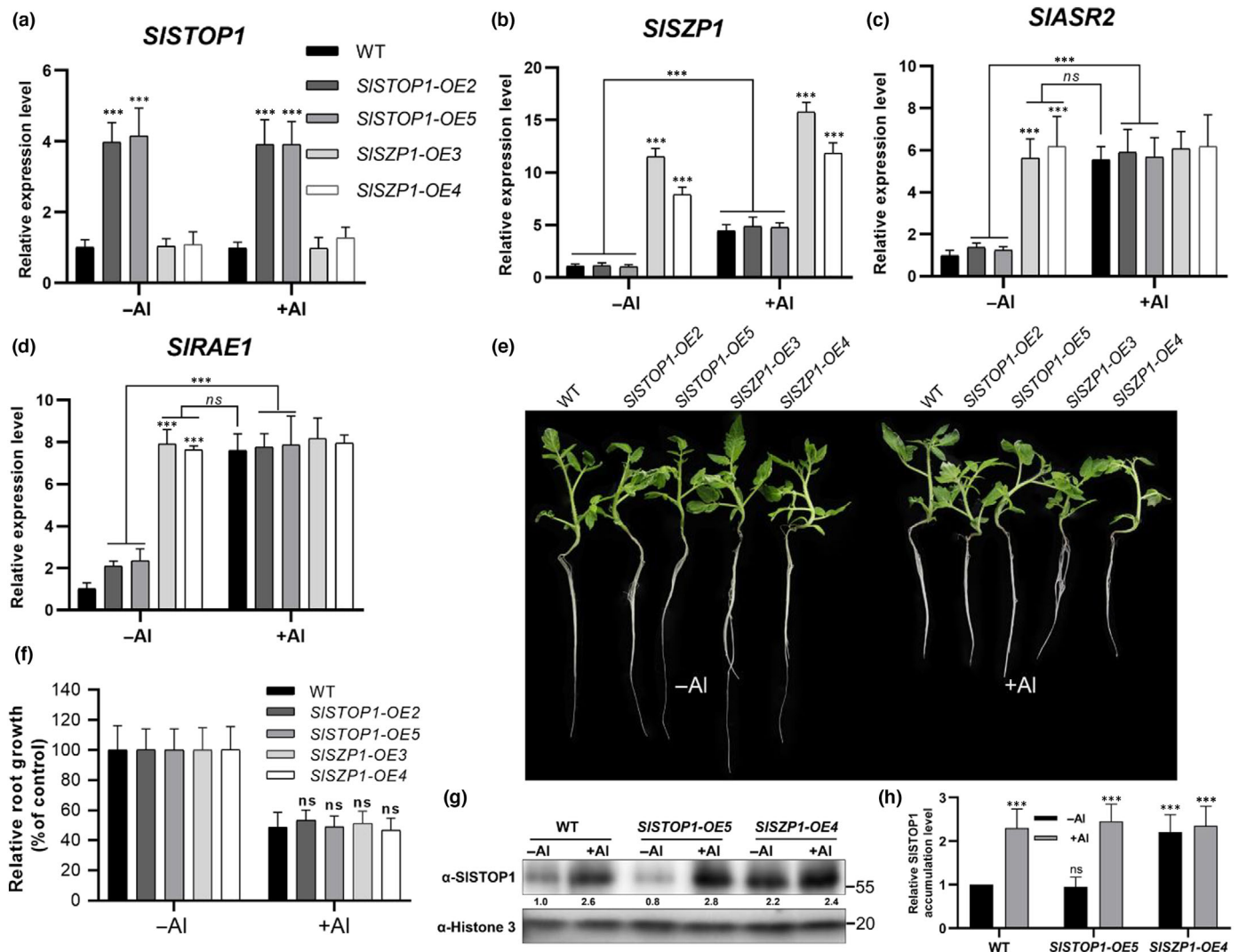
Fig. 7 Phenotypic analysis of *SlSTOP1* and *SlSZP1* overexpression lines. (a–d) Gene expression in wild-type (WT), *SlSTOP1-OE* and *SlSZP1-OE* lines. RT-PCR were used to determine the expression of *SlSTOP1* (a), *SlSZP1* (b), *SlASR2* (c) and *SlRAE1* (d) in the roots of 2-wk-old plants treated with/without $60\,\mu M$ $AlCl_3$ for 9 h (pH 4.7). Values are the mean $\pm$ SD ($n = 3$–4). 'ns' indicates no significant difference. Asterisks represent significant differences (*t*-test ***, $P < 0.001$). (e, f) Phenotype image (e) and quantitative data (f) of WT and overexpression (OE) lines. Here, 10-d-old plants were grown in modified Hoagland medium supplied with 0 or $30\,\mu M$ $AlCl_3$ (pH 4.5) for 10 d. Values are the mean $\pm$ SD ($n = 8$). (g, h) Five-week-old plants were treated with or without $60\,\mu M$ $AlCl_3$ for 9 h. The roots were sampled for nucleoprotein extraction. The same amount of crude protein was then detected using antibodies raised against SlSTOP1 and Histone 3 (g). The experiment was repeated three times and the SlSTOP1 accumulation was counted with IMAGEJ and normalised with Histone 3 (h). Values are the mean $\pm$ SD ($n = 3$). 'ns' indicates no significant difference. Asterisks represent significant differences (*t*-test $P < 0.001$).

encoding a C2H2-type zinc finger transcription factor in tomato. SlSTOP1 interacted with SlSZP1, also a C2H2-type transcription factor, and both *slstop1* and *slszp1* knockout mutants were hypersensitive to Al stress. SlSTOP1 directly bound to the promoter of Al-responsive genes, such as *SlRAE1* and *SlASR2*, while SlSZP1 did not bind to Al-responsive genes but increased their expression levels. Furthermore, the interaction between SlSTOP1 and SlSZP1 prevented SlSTOP1 from degradation by SlRAE1 (Fig. 8).

STOP1 is a well documented key Al-resistance gene in many species (Iuchi *et al.*, 2007; Yamaji *et al.*, 2009; Fan *et al.*, 2015), it has several copies in wheat and may have differential expression patterns in response to Al and proton (H^+) toxicity (Garcia-

Oliveira *et al.*, 2013; Fan *et al.*, 2016). In tomato, we identified *SlSTOP1* and its closest homologue Solyc06g065440, lacking the N- and C-termini activation domains (Fig. 1d,e) which were inhibited using Al treatments (Table S2). The transactivation domains are critical for the function of STOP1. We hypothesised that Solyc06g065440 may function through interaction with proteins with transactivation domains or just be a nonfunctional copy of SlSTOP1. In addition, AtSTOP2 and ART2 have also been described as STOP1 homologues in previous studies and act as minor isoforms of STOP1 (Kobayashi *et al.*, 2014; Che *et al.*, 2018). In tomato, *SlSTOP2*, an orthologue of *AtSTOP2* and *ART2*, was not induced using Al treatment, which is consistent with *AtSTOP2* but not with *ART2* (Table S2). Whether
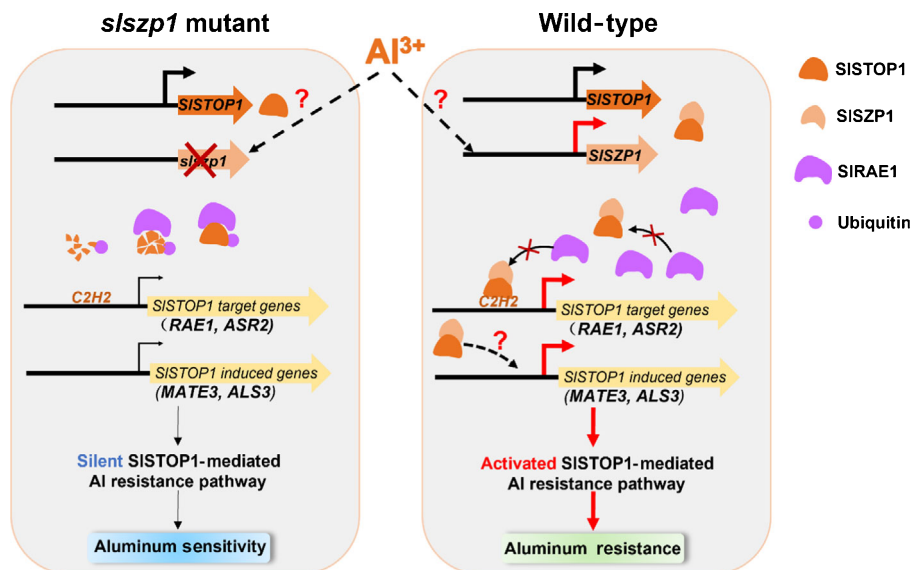
Fig. 8 Model for SlSTOP1 cooperating with SlSZP1 to detoxify aluminum (Al). In wild-type plants, Al stress induces the expression of SlSZP1. SlSZP1 then interacts with SlSTOP1, protecting SlSTOP1 from degradation by SlRAE1. The SlSTOP1–SlSZP1 complex induces the expression of Al resistance genes such as *SlASR2*, *SlMATE3* and *SlALS3*. The plants showed resistant to Al. In *slszp1* mutants, Al stress signals were not propagated through SlSZP1; SlSTOP1 is degraded through ubiquitination. The SlSTOP1-mediated Al resistance pathway was not expressed and the plants showed hypersensitive to Al. The grouped orange pieces represent degraded SlSTOP1. The red crosses mean nonexistent protein or inhibited actions. The thickness of the right arrows represents the different expression levels, arrows in red colour mean Al-induced gene expression and pathways.

SlSTOP2 also functions in Al resistance, as found for AtSTOP2, needs further investigation.

AtSTOP1 regulates plant Al tolerance mainly by regulating the expression of the organic acid transporter genes *ALMT1* and *MATE* (Sawaki *et al.*, 2009). Although *FRDL4*, a *MATE* family gene, was found as a ART1 downstream gene in rice, there is no evidence showing the regulation of *ALMTs* by ART1. In tomato, we found that *SlMATE3* expression was inhibited in *slstop1* mutants and that citrate exudation was also repressed. However, the expression of *ALMTs* was not found to be induced by Al stress. It has been shown previously that an indel in the *SlALMT9* promoter determined Al resistance in different tomato accessions (Ye *et al.*, 2017), therefore providing some basis towards the lack of *SlALMT9* induction by Al in our study. Moreover, ASRs, not found in Arabidopsis, were reported to be Al-responsible transcription factors in rice (Arenhart *et al.*, 2016). Here, we found that *SlASR2*, an *OsASR* homologue gene, was induced using Al treatments and directly activated by SlSTOP1. Our data and previous studies demonstrated that STOP1 and its orthologues played critical roles in plant Al tolerance and function through similar, albeit species-specific pathways. Based on the orthologue analysis of SlSZP1 by *OrthoDBv10.1*, SlSZP1-like proteins were found in many species, but not Arabidopsis (Fig. 1a). Possible causes are the differentiation of plants during evolution or that the search algorithm was missing from the *OrthoDB* database. Whether there is protein functionally like SlSZP1 in Arabidopsis requires further investigation.

Unlike the constitutive expression displayed by *SlSTOP1*, *SlSZP1* expression was induced by Al stress in WT and *slstop1* knockout mutants. Based on RNA-seq data, 448 *DRGs*, containing the key Al-induced genes *SlRAE1*, *SlAlS3*, *SlMATE3*

and *SlASR2*, were downregulated in both *slstop5-6* and *slszp22-1* mutants, indicating that SlSTOP1 and SlSZP1 play important and similar roles in plant Al resistance. In addition, single *slstop1* and *slszp1* knockouts and double *slstop1slszp1* knockout mutants displayed hypersensitivity to Al stress and the expression of SlSTOP1-regulated genes was similarly inhibited in all mutant lines (Figs 3c, 5). Notably, despite the inability of SlSZP1 to bind to SlSTOP1-regulated genes, their expression was inhibited in *slszp1* mutants (Fig. 5c–f). LUC/REN ratios indicated that the addition of SlSZP1 enhanced the expression of SlSTOP1 downstream genes (Fig. 5i–k). Due to the interaction between SlSZP1 and SlSTOP1, enhancement might result from a higher SlSTOP1 accumulation in tobacco leaves. Zinc finger domains are crucial for the binding capacity of the C2H2-type of transcription factors such as STOP1 (Tokizawa *et al.*, 2015) and mutations in one of these domains might result in the loss of its binding ability. STOP2, which contains only three zinc finger domains, and could only slightly activate some of the STOP1-regulated genes in Arabidopsis (Kobayashi *et al.*, 2014). It is possible that SlSZP1, containing only three zinc finger domains (instead of the four domains of STOP1), is unable to bind to the promoters of the genes targeted by SlSTOP1. Nevertheless, SlSZP1 still functions together with SlSTOP1 activating *SlASR2* and *SlRAE1*. Compared with the gene expression in WT under Al stress condition, 1651 *DRGs* were found in the *slszp22-1* mutant, which was even more than that in the *slstop5-6* mutant (1304 *DRGs*). These findings indicated that SlSZP1 may also regulate plant Al resistance by a SlSTOP1-independent pathway. Whether SlSZP1 can bind directly to specific downstream genes remains to be determined.

How Al affects STOP1 protein accumulation is an important and long-standing question. Recently, Zhang *et al.* (2019) reported that AtSTOP1 could be degraded by RAE1, a F-box domain E3-ligase. Nevertheless, the increase in RAE1 under Al stress did not affect STOP1 accumulation (Zhang *et al.*, 2019). HPR1 can sort STOP1 mRNA locations to affect STOP1 accumulation (Guo *et al.*, 2020). ESD4 (SMALL UBIQUITIN-LIKE MODIFIER (SUMO) protease) was shown to SUMOylate STOP1, affecting its function (Fang *et al.*, 2020). In this work, we found that the expression of *SlRAE1*, the orthologue of *AtRAE1* in tomato, was activated by SlSTOP1 and was induced by Al stress. SlRAE1, lacking the F-box domain, was able to interact with SlSTOP1 and SlSZP1, but the interaction with the full-length SlRAE1 could not be detected in yeast and tobacco. When *SlSTOP1* and *SlSZP1* were co-expressed together with *SlRAE1*, the interaction between SlSTOP1 and SlSZP1 was detected, suggesting that SlSZP1 protected SlSTOP1 from degradation by SlRAE1 and that the degradation pathway(s) might be conserved between species. *In vitro* pull-down assays showed that SlSZP1 might protect SlSTOP1 by competitively inhibiting the SlRAE1–SlSTOP1 interaction. A similar competitive protection mechanism was also reported in DELLA-GID1-NGR5 cassette regulating nitrogen-induced tiller growth and in the COP1-BBXs-HY5 cassette modulating hypocotyl elongation (Bursch *et al.*, 2020; Wu *et al.*, 2020). In addition, in the absence of Al, we found that SlSTOP1 accumulated in the WT, and *SlSZP1* mutations did not significantly diminish SlSTOP1 accumulation (Fig. 6g,h). Tokizawa *et al.* (2021) demonstrated that the phosphatidylinositol-specific phospholipase C (PI-PLC) pathway was involved in early STOP1 nuclear accumulation (Tokizawa *et al.*, 2021). We suspect that the PI-PLC pathway may also function to stabilise STOP1 in the absence of Al.

As the core factor of Al resistance, the *SlSTOP1* mutation silenced Al resistance genes both in the presence and absence of Al and caused an Al-sensitive phenotype (Figs 3c, 4b). Also, SlSTOP1 accumulation could not increase in *slszp1* mutants under Al stress conditions, therefore making the plants hypersensitive to Al stress, as seen in the *slstop1* mutants (Figs 3c, 6g). These results indicated that SlSZP1 was an essential factor maintaining SlSTOP1 accumulation under Al stress conditions. In addition, due to the unchanged *SlSZP1* expression levels between WT and *SlSTOP1-OEs* in the presence and absence of Al (Fig. 7a,b), overproduced SlSTOP1 protein might be degraded through the ubiquitin pathway in *SlSTOP1-OE* lines. Therefore, the expression of SlSTOP1 target genes and the phenotype of *SlSTOP1-OE* lines did not show any difference from that of WT (Fig. 7c–f). In *SlSZP-OE4*, SlSTOP1 accumulated under normal conditions, resulting in the activation of SlSTOP1 target genes (Fig. 7c,d,g). However, *SlSZP1-OE4* did not display higher amounts of SlSTOP1 than the WT, and the expression of *SlRAE1* and *SlASR2* was similar (Fig. 7c,d,g). Combined with the interaction among SlSTOP1, SlSZP1 and SlRAE1, the final levels of SlSTOP1 depends on both SlSTOP1 and SlSZP1 proteins, consequently, the aluminum resistance of plants cannot be improved with the overexpression of *SlSTOP1* and *SlSZP1*.

In conclusion, our results indicate that the interaction between SlSTOP1, SlSZP1 and SlRAE1 comprise a precise regulatory loop. Under Al stress conditions, SlSZP1 was induced and interacted with SlSTOP1 to maintain its stability. Then, the accumulation of SlSTOP1 activated Al-responsive genes, including *SlRAE1* (Fig. 8). Once Al was removed, *SlSZP1* expression decreased. The preaccumulation of SlRAE1 rapidly degraded highly accumulated SlSTOP1 and SlSZP1 proteins, returning Al-responsive genes to control levels. Finally, as the interaction of SlSTOP1 and SlSZP1 can promote the accumulation of SlSTOP1 and increase the expression of Al resistance genes, it might be worth testing whether elevating the expression of both *STOP1* and *SZP1* homologues can enhance the Al resistance in different species.

Competing interests

None declared.

Author contributions

Y-DG, NZ and LZ designed the project. LZ, DD, JW, ZW, JZ, R-YB, XW and MDMRW conducted the experiments. LZ, DD, JW, EB, NZ and Y-DG analysed the data and wrote the manuscript. All authors read and approved the final manuscript. LZ and DD contributed equally to this work.

ORCID

Eduardo Blumwald https://orcid.org/0000-0002-6449-6469
Yang-Dong Guo https://orcid.org/0000-0003-0564-9549

Data availability

Data available on request from the authors.

References

Arenhart RA, Bai Y, Valter de Oliveira LF, Bucker Neto L, Schunemann M, Maraschin FDS, Mariath J, Silverio A, Sachetto-Martins G, Margis R *et al.* 2014. New insights into aluminum tolerance in rice: the ASR5 protein binds

the *STAR1* promoter and other aluminum-responsive genes. *Molecular Plant* 7: 709–721.

Arenhart RA, Schunemann M, Bucker Neto L, Margis R, Wang Z-Y, Margis-Pinheiro M. 2016. Rice ASR1 and ASR5 are complementary transcription factors regulating aluminium responsive genes. *Plant, Cell & Environment* 39: 645–651.

Bose J, Babourina O, Shabala S, Rengel Z. 2010. Aluminium-induced ion transport in Arabidopsis: the relationship between Al tolerance and root ion flux. *Journal of Experimental Botany* 61: 3163–3175.

Bursch K, Toledo-Ortiz G, Pireyre M, Lohr M, Braatz C, Johansson H. 2020. Identification of BBX proteins as rate-limiting cofactors of HY5. *Nature Plants* 6: 921–928.

Cermak T, Curtin SJ, Gil-Humanes J, Cegan R, Kono TJY, Konecna E, Belanto JJ, Starker CG, Mathre JW, Greenstein RL *et al.* 2017. A multipurpose toolkit to enable advanced genome engineering in plants. *Plant Cell* 29: 1196–1217.

Che J, Tsutsui T, Yokosho K, Yamaji N, Ma JF. 2018. Functional characterization of an aluminum (Al)-inducible transcription factor, ART2, revealed a different pathway for Al tolerance in rice. *New Phytologist* 220: 209–218.

Chen H, Zou Y, Shang Y, Lin H, Wang Y, Cai R, Tang X, Zhou J-M. 2008. Firefly luciferase complementation imaging assay for protein–protein interactions in plants. *Plant Physiology* 146: 368–376.

Chow C-N, Lee T-Y, Hung Y-C, Li G-Z, Tseng K-C, Liu Y-H, Kuo P-L, Zheng H-Q, Chang W-C. 2019. PLANTPAN3.0: a new and updated resource for reconstructing transcriptional regulatory networks from ChIP-seq experiments in plants. *Nucleic Acids Research* 47(D1): D1155–D1163.

Fan W, Lou HQ, Gong YL, Liu MY, Cao MJ, Liu Y, Yang JL, Zheng SJ. 2015. Characterization of an inducible C2H2-type zinc finger transcription factor VuSTOP1 in rice bean (*Vigna umbellata*) reveals differential regulation between low pH and aluminum tolerance mechanisms. *New Phytologist* 208: 456–468.

Fan W, Lou HQ, Yang JL, Zheng SJ. 2016. The roles of STOP1-like transcription factors in aluminum and proton tolerance. *Plant Signaling & Behavior* 11: e1131371.

Fang Q, Zhang J, Zhang Y, Fan N, van den Burg HA, Huang C-F. 2020. Regulation of aluminum resistance in arabidopsis involves the SUMOylation of the zinc finger transcription factor STOP1. *Plant Cell* 32: 3921–3938.

Fernandez-Pozo N, Menda N, Edwards JD, Saha S, Tecle IY, Strickler SR, Bombarely A, Fisher-York T, Pujar A, Foerster H *et al.* 2015. The Sol Genomics Network (SGN)-from genotype to phenotype to breeding. *Nucleic Acids Research* 43(D1): D1036–D1041.

Garcia-Oliveira AL, Benito C, Prieto P, Menezes RA, Rodrigues-Pousada C, Guedes-Pinto H, Martins-Lopes P. 2013. Molecular characterization of TaSTOP1 homoeologues and their response to aluminium and proton (H+) toxicity in bread wheat (*Triticum aestivum* L.). *BMC Plant Biology* 13: 134–146.

Garcia-Oliveira AL, Martins-Lopes P, Tolra R, Poschenrieder C, Tarquis M, Guedes-Pinto H, Benito C. 2014. Molecular characterization of the citrate transporter gene *TaMATE1* and expression analysis of upstream genes involved in organic acid transport under Al stress in bread wheat (*Triticum aestivum*). *Physiologia Plantarum* 152: 441–452.

Guo JL, Zhang Y, Gao HL, Li SB, Wang ZY, Huang CF. 2020. Mutation of HPR1encoding a component of the THO/TREX complex reduces STOP1 accumulation and aluminium resistance in *Arabidopsis thaliana*. *New Phytologist* 228: 179–193.

Hoekenga OA, Maron LG, Pineros MA, Cancado GMA, Shaff J, Kobayashi Y, Ryan PR, Dong B, Delhaize E, Sasaki T *et al.* 2006. AtALMT1, which encodes a malate transporter, is identified as one of several genes critical for aluminum tolerance in Arabidopsis. *Proceedings of the National Academy of Sciences, USA* 103: 9738–9743.

Huang C-F. 2021. Activation and activity of STOP1 in aluminium resistance. *Journal of Experimental Botany* 72: 2269–2272.

Huang C-F, Yamaji N, Chen Z, Ma JF. 2012. A tonoplast-localized half-size ABC transporter is required for internal detoxification of aluminum in rice. *The Plant Journal* 69: 857–867.

Huang CF, Yamaji N, Mitani N, Yano M, Nagamura Y, Ma JF. 2009. A bacterial-type ABC transporter is involved in aluminum tolerance in rice. *Plant Cell* 21: 655–667.

Iuchi S, Koyama H, Iuchi A, Kobayashi Y, Kitabayashi S, Kobayashi Y, Ikka T, Hirayama T, Shinozaki K, Kobayashi M. 2007. Zinc finger protein STOP1 is critical for proton tolerance in Arabidopsis and coregulates a key gene in aluminum tolerance. *Proceedings of the National Academy of Sciences, USA* 104: 9900–9905.

Jin JF, He QY, Li PF, Lou HQ, Chen WW, Yang JL. 2021. Genome-wide identification and gene expression analysis of acyl-activating enzymes superfamily in tomato (*Solanum lycopersicum*) under aluminum stress. *Frontiers in Plant Science* 12: 754147.

Jin JF, Wang ZQ, He QY, Wang JY, Li PF, Xu JM, Zheng SJ, Fan W, Yang JL. 2020. Genome-wide identification and expression analysis of the NAC transcription factor family in tomato (*Solanum lycopersicum*) during aluminum stress. *BMC Genomics* 21: 288–301.

Kibria MG, Barton L, Rengel Z. 2021. Genetic aluminium resistance coupled with foliar magnesium application enhances wheat growth in acidic soil. *Journal of the Science of Food and Agriculture* 101: 4643–4652.

Kobayashi Y, Ohyama Y, Kobayashi Y, Ito H, Iuchi S, Fujita M, Zhao C-R, Tanveer T, Ganesan M, Kobayashi M *et al.* 2014. STOP2 activates transcription of several genes for Al- and low pH-tolerance that are regulated by STOP1 in Arabidopsis. *Molecular Plant* 7: 311–322.

Langmead B, Trapnell C, Pop M, Salzberg SL. 2009. Ultrafast and memory-efficient alignment of short DNA sequences to the human genome. *Genome Biology* 10: R25.

Larsen PB, Geisler MJB, Jones CA, Williams KM, Cancel JD. 2005. ALS3 encodes a phloem-localized ABC transporter-like protein that is required for aluminum tolerance in Arabidopsis. *The Plant Journal* 41: 353–363.

Li B, Dewey CN. 2011. RSEM: accurate transcript quantification from RNA-Seq data with or without a reference genome. *BMC Bioinformatics* 12: 322–328.

Li H, Durbin R. 2009. Fast and accurate short read alignment with Burrows-Wheeler transform. *Bioinformatics* 25: 1754–1760.

Liang CY, Pineros MA, Tian J, Yao ZF, Sun LL, Liu JP, Shaff J, Coluccio A, Kochian LV, Liao H. 2013. Low pH, Aluminum, and phosphorus coordinately regulate malate exudation through GmALMT1 to improve soybean adaptation to acid soils. *Plant Physiology* 161: 1347–1361.

Ligaba-Osena A, Fei ZJ, Liu JP, Xu YM, Shaff J, Lee SC, Luan S, Kudla J, Kochian L, Pineros M. 2017. Loss-of-function mutation of the calcium sensor CBL1 increases aluminum sensitivity in Arabidopsis. *New Phytologist* 214: 830–841.

Liu J, Magalhaes JV, Shaff J, Kochian LV. 2009. Aluminum-activated citrate and malate transporters from the MATE and ALMT families function independently to confer Arabidopsis aluminum tolerance. *The Plant Journal* 57: 389–399.

Ma JF, Ryan PR, Delhaize E. 2001. Aluminium tolerance in plants and the complexing role of organic acids. *Trends in Plant Science* 6: 273–278.

Magalhaes JV, Liu J, Guimaraes CT, Lana UGP, Alves VMC, Wang YH, Schaffert RE, Hoekenga OA, Pineros MA, Shaff JE *et al.* 2007. A gene in the multidrug and toxic compound extrusion (*MATE*) family confers aluminum tolerance in sorghum. *Nature Genetics* 39: 1156–1161.

Matsumoto H, Riechers DE, Lygin AV, Baluska F, Sivaguru M. 2015. Aluminum signaling and potential links with safener-induced detoxification in plants. In: Panda, SK, Baluska, F, eds. *Aluminum stress adaptation in plants, vol. 24*. Berlin, Germany: Springer, 1–35.

Munoz A, Mar CM. 2018. Coimmunoprecipitation of interacting proteins in plants. In: McDonald PN, ed. *Two-hybrid systems: methods and protocols, vol. 1794*. Clifton, NJ, USA: Methods in Molecular Biology, 279–287.

Ohyama Y, Ito H, Kobayashi Y, Ikka T, Morita A, Kobayashi M, Imaizumi R, Aoki T, Komatsu K, Sakata Y *et al.* 2013. Characterization of AtSTOP1 orthologous genes in tobacco and other plant species. *Plant Physiology* 162: 1937–1946.

Poschenrieder C, Gunse B, Corrales I, Barcelo J. 2008. A glance into aluminum toxicity and resistance in plants. *Science of the Total Environment* 400: 356–368.

Ryan PR, Shaff JE, Kochian LV. 1992. Aluminum toxicity in roots - correlation among ionic currents, ion fluxes, and root elongation in aluminum-sensitive and aluminum-tolerant wheat cultivars. *Plant Physiology* 99: 1193–1200.

Sadhukhan A, Kobayashi Y, Iuchi S, Koyama H. 2021. Synergistic and antagonistic pleiotropy of STOP1 in stress tolerance. *Trends in Plant Science* 26: 1014–1022.

Sanchez PA, Salinas JG. 1981. Low-input technology for managing oxisols and ultisols in tropical America. *Advances in Agronomy* 34: 279–406.

dos Santos AL, Chaves-Silva S, Yang L, Maia LGS, Chalfun-Junior A, Sinharoy S, Zhao J, Benedito VA. 2017. Global analysis of the *MATE* gene family of metabolite transporters in tomato. *BMC Plant Biology* 17: 185–197.

Sasaki T, Yamamoto Y, Ezaki B, Katsuhara M, Ahn SJ, Ryan PR, Delhaize E, Matsumoto H. 2004. A wheat gene encoding an aluminum-activated malate transporter. *The Plant Journal* 37: 645–653.

Sawaki Y, Iuchi S, Kobayashi Y, Kobayashi Y, Ikka T, Sakurai N, Fujita M, Shinozaki K, Shibata D, Kobayashi M *et al.* 2009. STOP1 regulates multiple genes that protect Arabidopsis from proton and aluminum toxicities. *Plant Physiology* 150: 281–294.

Shaff JE, Schultz BA, Craft EJ, Clark RT, Kochian LV. 2010. GEOCHEM-EZ: a chemical speciation program with greater power and flexibility. *Plant and Soil* 330: 207–214.

Singh SP, Singh Z, Swinny EE. 2009. Sugars and organic acids in Japanese plums (*Prunus salicina* Lindell) as influenced by maturation, harvest date, storage temperature and period. *International Journal of Food Science and Technology* 44: 1973–1982.

Sun HJ, Uchii S, Watanabe S, Ezura H. 2006. A highly efficient transformation protocol for Micro-Tom, a model cultivar for tomato functional genomics. *Plant and Cell Physiology* 47: 426–431.

Tarazona S, Garcia-Alcalde F, Dopazo J, Ferrer A, Conesa A. 2011. Differential expression in RNA-seq: a matter of depth. *Genome Research* 21: 2213–2223.

Tokizawa M, Enomoto T, Ito H, Wu L, Kobayashi Y, Mora-Macias J, Armenta-Medina D, Iuchi S, Kobayashi M, Nomoto M *et al.* 2021. High affinity promoter binding of STOP1 is essential for early expression of novel aluminum-induced resistance genes *GDH1* and *GDH2* in Arabidopsis. *Journal of Experimental Botany* 72: 2769–2789.

Tokizawa M, Kobayashi Y, Saito T, Kobayashi M, Iuchi S, Nomoto M, Tada Y, Yamamoto YY, Koyama H. 2015. SENSITIVE TO PROTON RHIZOTOXICITY1, CALMODULIN BINDING TRANSCRIPTION ACTIVATOR2, and other transcription factors are involved in *aluminum-activated malate transporter1* expression. *Plant Physiology* 167: 991–1003.

Tsutsui T, Yamaji N, Ma JF. 2011. Identification of a cis-acting element of ART1, a C2H2-type zinc-finger transcription factor for aluminum tolerance in rice. *Plant Physiology* 156: 925–931.

Urbanczyk-Wochniak E, Fernie AR. 2005. Metabolic profiling reveals altered nitrogen nutrient regimes have diverse effects on the metabolism of hydroponically-grown tomato (*Solanum lycopersicum*) plants. *Journal of Experimental Botany* 56: 309–321.

Wang JF, Zhang L, Cao YY, Qi CD, Li ST, Liu L, Wang GL, Mao AJ, Ren SX, Guo YD. 2018. CsATAF1 positively regulates drought stress tolerance by an ABA-dependent pathway and by promoting ROS scavenging in cucumber. *Plant and Cell Physiology* 59: 930–945.

Wu K, Wang S, Song W, Zhang J, Wang Y, Liu Q, Yu J, Ye Y, Li S, Chen J *et al.* 2020. Enhanced sustainable green revolution yield via nitrogen-responsive chromatin modulation in rice. *Science* 367: 367–375.

Wu XX, Li R, Shi J, Wang JF, Sun QQ, Zhang HJ, Xing YX, Qi Y, Zhang N, Guo YD. 2014. *Brassica oleracea* MATE encodes a citrate transporter and enhances aluminum tolerance in *Arabidopsis thaliana*. *Plant and Cell Physiology* 55: 1426–1436.

Xia J, Yamaji N, Kasai T, Ma JF. 2010. Plasma membrane-localized transporter for aluminum in rice. *Proceedings of the National Academy of Sciences, USA* 107: 18381–18385.

Yamaji N, Huang CF, Nagao S, Yano M, Sato Y, Nagamura Y, Ma JF. 2009. A zinc finger transcription factor ART1 regulates multiple genes implicated in aluminum tolerance in rice. *Plant Cell* 21: 3339–3349.

Yan LH, Wei SW, Wu YR, Hu RL, Li HJ, Yang WC, Xie Q. 2015. High-efficiency genome editing in Arabidopsis using YAO promoter-driven CRISPR/Cas9 system. *Molecular Plant* 8: 1820–1823.

Ye J, Wang X, Hu TX, Zhang FX, Wang B, Li CX, Yang TX, Li HX, Lu YG, Giovannoni JJ *et al.* 2017. An InDel in the promoter of Al-ACTIVATED MALATE TRANSPORTER9 selected during tomato domestication determines fruit malate contents and aluminum tolerance. *Plant Cell* 29: 2249–2268.

Yokosho K, Ma JF. 2015. Transcriptional regulation of al tolerance in plants. In: Panda SK, Baluska F, eds. *Aluminum stress adaptation in plants, vol. 24*. Berlin, Germany: Springer, 37–46.

Zhang L, Wu XX, Wang JF, Qi CD, Wang XY, Wang GL, Li MY, Li XS, Guo YD. 2018. BoALMT1, an Al-induced malate transporter in cabbage, enhances aluminum tolerance in *Arabidopsis thaliana*. *Frontiers in Plant Science* 8: 02156.

Zhang Y, Chen M, Siemiatkowska B, Toleco MR, Jing Y, Strotmann V, Zhang J, Stahl Y, Fernie AR. 2020. A highly efficient agrobacterium-mediated method for transient gene expression and functional studies in multiple plant species. *Plant Communications* 1: 100028.

Zhang Y, Zhang J, Guo JL, Zhou FL, Singh S, Xu X, Xie Q, Yang ZB, Huang CF. 2019. F-box protein RAE1 regulates the stability of the aluminum-resistance transcription factor STOP1 in Arabidopsis. *Proceedings of the National Academy of Sciences, USA* 116: 319–327.

Zhu XF, Lei GJ, Wang ZW, Shi YZ, Braam J, Li GX, Zheng SJ. 2013. Coordination between apoplastic and symplastic detoxification confers plant aluminum resistance. *Plant Physiology* 162: 1947–1955.

Supporting Information

Additional Supporting Information may be found online in the Supporting Information section at the end of the article.

Fig. S1 Fundamental analysis of SlSTOP1.

Fig. S2 Identification of *SlSTOP1* and *SlSZP1* knockout mutants.

Fig. S3 SlSTOP1 directly regulates *SlASR2* expression.

Fig. S4 The binding assay of SlSTOP1 or SlSZP1 to Al-responsive genes.

Fig. S5 Gene expression in wild-type (WT) under different conditions.

Fig. S6 SlSTOP1 interacts with SlRAE1.

Table S1 Lists of primers and vectors used in this study.

Table S2 Fragments per kilobase of transcript per million mapped reads (FPKM) of 42 differentially expressed genes between wild-type and *slstop5-6* in RNA-seq data.

Please note: Wiley Blackwell are not responsible for the content or functionality of any Supporting Information supplied by the authors. Any queries (other than missing material) should be directed to the *New Phytologist* Central Office.